

Benchmarking the Semi-Stochastic $CC(P;Q)$ Approach for Singlet–Triplet Gaps in Biradicals

Arnab Chakraborty,¹ Stephen H. Yuwono,¹ J. Emiliano Deustua,¹ Jun Shen,¹ and Piotr Piecuch^{1,2, a)}

¹*Department of Chemistry, Michigan State University, East Lansing, Michigan 48824, USA*

²*Department of Physics and Astronomy, Michigan State University, East Lansing, Michigan 48824, USA*

(Dated: 4 October 2022)

We recently proposed a semi-stochastic approach to converging high-level coupled-cluster (CC) energetics, such as those obtained in the CC calculations with singles, doubles, and triples (CCSDT), in which the deterministic $CC(P;Q)$ framework is merged with the stochastic configuration interaction Quantum Monte Carlo propagations [J. E. Deustua, J. Shen, and P. Piecuch, *Phys. Rev. Lett.* **119**, 223003 (2017)]. In this work, we investigate the ability of the semi-stochastic $CC(P;Q)$ methodology to recover the CCSDT energies of the lowest singlet and triplet states and the corresponding singlet–triplet gaps of biradical systems using methylene, $(\text{HFH})^-$, cyclobutadiene, cyclopentadienyl cation, and trimethylenemethane as examples.

I. INTRODUCTION

There has been great progress in *ab initio* computational quantum chemistry, but an accurate description of multi-reference (MR) situations, such as molecular potential energy surfaces along bond breaking coordinates, electronic spectra of radical and biradical species, and excited states dominated by two-electron transitions, continues to represent a major challenge. While a traditional way of addressing this challenge has been to use MR approaches that rely on multi-dimensional model spaces spanned by multiple reference determinants,^{1–8} in this work we focus on methods based on the single-reference (SR) coupled-cluster (CC) theory^{9–13} (cf. Refs. 14 and 15 for selected reviews), in which the ground electronic state is expressed using the exponential wave function ansatz $|\Psi\rangle = e^T |\Phi\rangle$, where $T = \sum_{n=1}^N T_n$ is the cluster operator, N is the total number of correlated electrons in the system, T_n is the n -body (n -particle– n -hole or n -tuply excited) component of T , and $|\Phi\rangle$ is the reference determinant that serves as a Fermi vacuum. By truncating T at various excitation ranks, one obtains the well-known hierarchy of SRCC approximations, including the CC method with singles and doubles (CCSD),^{16–19} where T is truncated at T_2 , the CC method with singles, doubles, and triples (CCSDT),^{20–23} where T is truncated at T_3 , the CC method with singles, doubles, triples, and quadruples (CCSDTQ),^{24–27} where T is truncated at T_4 , and so on. As long as the number of strongly correlated electrons is not too large, the CCSD, CCSDT, CCSDTQ, etc. hierarchy and its extensions to excited states and properties other than energy via the equation-of-motion (EOM)^{28–35} and linear response (LR)^{36–44} CC frameworks rapidly converge to the exact, full configuration interaction (FCI), limit.¹⁵ As a result, the CCSDT, CCSDTQ, and similar methods and their EOM and LR

extensions are capable of accurately describing typical MR situations, such as bond rearrangements in chemical reactions, singlet–triplet gaps in biradicals, and excited states having substantial double excitation character, via particle–hole excitations from a single determinant.

The convergence of the CCSD, CCSDT, CCSDTQ, etc. hierarchy toward FCI in the majority of chemical applications is fast, but to achieve a quantitative description, one has to go beyond the basic CCSD level and face high, often prohibitive, computational costs, such as the iterative $n_o^3 n_u^5$ steps of CCSDT or the even more demanding $n_o^4 n_u^6$ steps of CCSDTQ (n_o and n_u are the numbers of correlated occupied and unoccupied orbitals, respectively). Thus, one of the key challenges in the development of SRCC methodologies has been the incorporation of many-electron correlation effects due to higher-than-two-body components of the cluster operator T without running into the enormous computational costs of the high-level parent methods, such as CCSDT or CCSDTQ, while avoiding the failures of perturbative approximations of the CCSD(T)^{45,46} type when bond breaking, biradicals, and other MR situations are examined.^{14,15,47–49}

One of the most promising ways of addressing the above challenge within the SRCC framework is offered by the $CC(P;Q)$ formalism, which allows one to correct the CC and EOMCC energies obtained using conventional as well as unconventional truncations in the cluster and EOM excitation operators for the missing many-electron correlation effects of interest using the moment expansions developed in Refs. 50–53. Focusing on the ground electronic states (or, in general, the lowest states of symmetries of interest, as in the case of many lowest-energy singlet, doublet, or triplet states), the $CC(P;Q)$ methods based on correcting the CC energies obtained with the conventional truncations in T at a given excitation rank reduce to the left-eigenstate completely renormalized (CR) CC approaches, such as CR-CC(2,3),^{54–58} in which one corrects the CCSD energies for the leading T_3 correlations, and its higher-order extensions.^{53,59–62} The CR-CC(2,3) method improves

^{a)}Corresponding author; e-mail: piecuch@chemistry.msu.edu.

poor performance of CCSD(T) in situations involving covalent bond breaking^{50,54–57,60,63,64} and certain types of noncovalent interactions,^{59,65} while retaining the relatively inexpensive iterative $n_o^2 n_u^4$ and noniterative $n_o^3 n_u^4$ steps of CCSD(T), but neither CR-CC(2,3) nor its CR-CCSD(T)^{47,48,66,67} and locally renormalized CCSD(T)⁶⁸ predecessors, nor their CCSD(2)_T,^{69–72} CCSD(T)_Λ,^{73–75} Λ-CCSD(T),^{76,77} and CCSD(T- n)^{78,79} counterparts, designed to improve CCSD(T) as well, are accurate enough when the coupling of the low-order T_n components, such as T_1 and T_2 , and their higher-order counterparts with $n > 2$, e.g., T_3 , becomes larger.^{51,52} One can address this issue by solving for T_1 and T_2 clusters in the presence of the dominant higher-than-doubly excited components of T identified with the help of active orbitals, as in the CCSDt, CCSDtq, and similar schemes,^{27,31,32,49,80–85} and account for the remaining correlation effects of interest (e.g., the T_3 correlations not captured by CCSDt) using the CC($P;Q$) moment expansions, but the resulting CC(t;3), CC(t,q;3), CC(t,q;3,4), etc. hierarchy,^{50–53,59,65} while accurately reproducing the parent CCSDT and CCSDTQ energetics at the fraction of the computational costs, requires choosing user- and system-dependent active orbitals. The question arises if the CC($P;Q$) methodology can be similarly successful without having to define active orbitals tuned to a given calculation.

To address this question, we have recently proposed an automated way of identifying the leading T_n components with $n > 2$ within the CC($P;Q$) framework by merging the deterministic CC($P;Q$) formalism with the stochastic configuration interaction (CI) Quantum Monte Carlo (QMC)^{86–90} and CC Monte Carlo (CCMC)^{91–94} propagations.^{95–97} As shown in Ref. 95, the results of the semi-stochastic CC($P;Q$) computations, in which the lists of determinants needed to define higher-than-doubly excited cluster components are extracted from the FCIQMC and CCSDT-MC runs, rapidly converge to the parent high-level CC energetics, represented in Ref. 95 by CCSDT, out of the early stages of the underlying QMC propagations, even when electronic quasi-degeneracies and the associated T_3 correlations become substantial. In more recent studies, it has been demonstrated that the semi-stochastic CC($P;Q$) calculations exhibit a similarly fast convergence toward the parent CCSDT and CCSDTQ energies when the FCIQMC propagations are replaced by their less expensive truncated CISDT-MC and CISDTQ-MC analogs⁹⁷ and that the CIQMC-driven CC($P;Q$) framework can be very effective in converging the EOMCCSDT energies of excited states, including states of the same symmetry as the ground state, states of different symmetries, and challenging excited states dominated by two-electron transitions⁹⁶ (cf., also, Ref. 98). Our group has also explored the deterministic alternative to the semi-stochastic CC($P;Q$) methodology by replacing the CIQMC and CCMC propagations, needed to identify the dominant higher-than-doubly excited components of T , by the sequences of Hamiltonian diagonalizations defining the selected CI approach abbreviated as

CIQMC,^{99–101} obtaining encouraging results.¹⁰²

In the present work, we investigate the ability of the semi-stochastic CC($P;Q$) formalism, driven by either FCIQMC or CISDTQ-MC propagations, to converge the energies of the lowest singlet and triplet states and the corresponding singlet-triplet gaps, ΔE_{S-T} , resulting from the high-level CCSDT calculations for the selected organic biradicals, including methylene, cyclobutadiene, cyclopentadienyl cation, and trimethylenemethane, and a prototype magnetic system, represented by the (HFH)⁻ ion. Understanding electronic structure and properties of organic biradicals is of major significance in areas such as chemical reaction dynamics,¹⁰³ molecular magnetism,¹⁰⁴ spintronics,^{105,106} nonlinear optics,¹⁰⁷ photochemical pathways,^{108–110} and photovoltaics.^{111–113} The linear (HFH)⁻ species, in which one simultaneously stretches both H-F bonds, is a model inorganic magnetic system, in which two paramagnetic centers carrying unpaired spins associated with the terminal hydrogen atoms are coupled via a polarizable diamagnetic bridge formed by F⁻.¹¹⁴ It is well established that an accurate determination of the ordering of the low-lying singlet and triplet states and ΔE_{S-T} values in biradicals, which are among their most important physical characteristics, remains a significant challenge for computational quantum chemistry, even when high-level *ab initio* wave function methods are used in the calculations.^{52,57,115–126} This is because one has to balance substantial nondynamical correlation effects needed for an accurate description of the low-spin singlet state, which can be either of the open-shell type involving the nearly degenerate singly occupied valence molecular orbitals (MOs) or of the multi-configurational type mixing two closed-shell determinants involving the highest occupied and lowest unoccupied MOs, HOMO and LUMO, respectively [the determinant in which HOMO is doubly occupied and the doubly excited determinant of the (HOMO)² → (LUMO)² type], with the dynamical correlations of the high-spin triplet state, which has a predominantly SR character. If we limit ourselves to the black-box SRCC methodologies, the only methods that can provide a reliable and balanced description of the lowest singlet and triplet states and singlet-triplet gaps in biradicals and magnetic systems are the high-level CC approaches, beginning with CCSDT, and their particle-nonconserving double electron-attachment (DEA) and double ionization potential (DIP) EOMCC counterparts,^{123,125–136} especially those that incorporate the high-rank 4-particle-2-hole (4p2h) and 4-hole-2-particle (4h2p) correlations on top of the CC treatment of the underlying closed-shell cores.^{123,125,126,135,136} It is interesting to examine if our semi-stochastic, CIQMC-driven, CC($P;Q$) methodology can be as successful in recovering the CCSDT results for the lowest singlet and triplet states and ΔE_{S-T} gaps of the biradical and magnetic systems listed above as in the previously reported benchmark studies of bond dissociations,^{95,97} chemical reaction pathways,^{95,97} and excited electronic states.⁹⁶

II. THEORY

We recall that the $CC(P;Q)$ formalism is a natural generalization of the biorthogonal moment expansions of Refs. 54–56, which in the past resulted in the CR-CC/EOMCC triples corrections to the CCSD/EOMCCSD energies, such as CR-CC(2,3),^{54–58} CR-EOMCC(2,3),^{56,137} and δ -CR-EOMCC(2,3),¹³⁸ and their extensions to quadruples,^{53,59–62} to unconventional truncations in the cluster and EOM excitation operators. In the case of the ground electronic state, or the lowest-energy state of symmetry other than the ground state that can be treated using the SRCC framework, the $CC(P;Q)$ calculation is a two-step procedure. In the first step, abbreviated as $CC(P)$, we solve the CC amplitude equations in the subspace of the many-electron Hilbert space, $\mathcal{H}^{(P)}$, referred to as the P space, spanned by the excited determinants that together with the reference determinant $|\Phi\rangle$ dominate the target state $|\Psi\rangle$ of interest, for the suitably truncated form of the cluster operator T consistent with the content of the P space, designated as $T^{(P)}$, and the corresponding energy $E^{(P)}$. In the second step, we correct the $CC(P)$ energy $E^{(P)}$ for the many-electron correlation effects captured with the help of the excited determinants that span another subspace of the Hilbert space, called the Q space and denoted as $\mathcal{H}^{(Q)}$, using the noniterative correction $\delta(P;Q)$ derived from the $CC(P;Q)$ moment expansion introduced in Refs. 50–52. The final $CC(P;Q)$ energy is determined as

$$E^{(P+Q)} = E^{(P)} + \delta(P;Q), \quad (1)$$

where the explicit formulas for the correction $\delta(P;Q)$ in terms of the generalized moments^{66,67,139} of the $CC(P)$ equations, which correspond to projections of these equations on the complementary Q -space determinants, and the left eigenstate $\langle\Phi|(1 + \Lambda^{(P)})$ of the similarity-transformed Hamiltonian $\overline{H}^{(P)} = e^{-T^{(P)}} H e^{T^{(P)}}$ in the P space, with $\Lambda^{(P)}$ representing the relevant hole–particle deexcitation operator, can be found in Refs. 50–53 (see, also, Refs. 59, 65, 95–97, and 102). In the most complete variant of the $CC(P;Q)$ formalism adopted in this work, one uses the Epstein–Nesbet denominators involving $\overline{H}^{(P)}$ in determining the $\delta(P;Q)$ corrections. One could employ the Møller–Plesset denominators instead, but the Epstein–Nesbet form has been shown to be generally more accurate (see, e.g., Refs. 52, 53, 95, and 97).

The main advantage of the $CC(P;Q)$ formalism compared to its CR-CC predecessors is the flexibility in defining the underlying P and Q spaces that allows us to relax the lower-order T_1 and T_2 components of the cluster operator T in the presence of their higher-order counterparts, such as the leading T_3 contributions, which the CR-CC(2,3), CCSD(2)_T, Λ -CCSD(T), and other noniterative triples corrections to CCSD cannot do. As explained in the Introduction, one can incorporate the coupling among the lower-rank T_1 and T_2 and higher-rank T_n components with $n > 2$ within the $CC(P;Q)$ frame-

work by including the dominant higher-than-doubly excited determinants identified with the help of active orbitals or selected CI diagonalizations in the P space, using the $\delta(P;Q)$ corrections to capture the remaining correlations of interest, but this is not what we do in this work. Here, we explore the alternative approach that utilizes the semi-stochastic $CC(P;Q)$ methodology of Refs. 95–97, in which the leading higher-than-doubly excited determinants included in the underlying P spaces are identified using CIQMC runs, whereas the corresponding Q spaces, needed to determine corrections $\delta(P;Q)$, are populated by the remaining determinants of interest not captured by CIQMC at a given propagation time τ . Given our interest in converging the CCSDT energies of the lowest singlet and triplet states of biradical systems, we adopt in this study the following $CC(P;Q)$ algorithm:

1. Initiate the desired CIQMC (in this study, FCIQMC or CISDTQ-MC) propagation by placing a certain number of walkers on the appropriate reference determinant $|\Phi\rangle$. In calculations for the lowest singlet states of symmetries of interest, we used the relevant restricted Hartree–Fock (RHF) determinants as reference functions. In the case of the lowest triplet states, we used the restricted open-shell Hartree–Fock (ROHF) references.
2. After a certain number of CIQMC time steps, referred to as MC iterations, or, equivalently, at some propagation time $\tau > 0$, extract a list of triply excited determinants captured by CIQMC, i.e., those triples that are populated by at least one walker.
3. Solve the $CC(P)$ amplitude equations and the associated left eigenstate problem involving $\overline{H}^{(P)}$ in the P space spanned by all singly and doubly excited determinants and the subset of triply excited determinants identified in step 2, using the same reference $|\Phi\rangle$ as that chosen to initiate the CIQMC run, to obtain the cluster operator $T^{(P)}$, defined as $T_1 + T_2 + T_3^{(\text{MC})}$, and its $\Lambda^{(P)} = \Lambda_1 + \Lambda_2 + \Lambda_3^{(\text{MC})}$ companion, where the list of triples in $T_3^{(\text{MC})}$ and $\Lambda_3^{(\text{MC})}$ is extracted from the CIQMC propagation at time τ . Calculate the energy $E^{(P)}$.
4. Correct the $CC(P)$ energy $E^{(P)}$ obtained in step 3 for the remaining T_3 correlations using Eq. (1), where the Q space needed to determine the $\delta(P;Q)$ correction consists of the triply excited determinants not captured by the CIQMC propagation at time τ , to obtain the $CC(P;Q)$ energy $E^{(P+Q)}$.
5. Repeat steps 2–4 at some later CIQMC propagation time $\tau' > \tau$ to check the convergence of the $CC(P;Q)$ energies $E^{(P+Q)}$. Stop the calculation if the consecutive $E^{(P+Q)}$ values do not change within an *a priori* defined convergence threshold or if the stochastically determined P space captures

a large enough fraction of the triply excited determinants sufficient to achieve the desired accuracy relative to the parent CCSDT approach.

In this work, we explored two types of CIQMC propagations to carry out our semi-stochastic $CC(P;Q)$ computations. For smaller systems, including methylene, $(\text{HFH})^-$, and cyclobutadiene, we used FCIQMC, which allows the CIQMC algorithm to explore the entire many-electron Hilbert space. For the two largest biradical species considered in our calculations, namely, cyclopentadienyl cation and trimethylenemethane, we used the truncated CISDTQ-MC approach, in which spawning beyond quadruply excited determinants relative to reference $|\Phi\rangle$ is disallowed, reducing computation costs compared to FCIQMC, especially in later stages of CIQMC propagations. As shown in Ref. 97, convergence of the $CC(P;Q)$ energies toward their high-level CC parents, such as CCSDT, is not affected by the type of the CIQMC approach used to identify the relevant higher-than-doubly excited determinants (in this work, the triply excited determinants), so choosing CISDTQ-MC as a substitute for FCIQMC has no effect on our conclusions. Following our earlier studies of the semi-stochastic $CC(P;Q)$ methodology^{95–97} and related work,⁹⁸ in all of the CIQMC calculations reported in this article, we relied on the initiator CIQMC (*i*-CIQMC) algorithm introduced in Ref. 87, based on integer walker numbers, in which only the determinants populated by n_a or more walkers are allowed to spawn new walkers onto empty determinants, but the semi-stochastic $CC(P;Q)$ procedure summarized above is flexible and could be merged with other CIQMC techniques developed in recent years, such as those described in Refs. 89 and 90. While the convergence of the $CC(P;Q)$ energies of the lowest singlet and triplet states of biradicals considered in this study and of the corresponding singlet–triplet gaps obtained with the help of *i*-CIQMC propagations toward the parent CCSDT results is very fast, we will examine the utility of the newer CIQMC algorithms in the future work.

As explained in Refs. 95–97 (cf., also, Ref. 98), the semi-stochastic $CC(P;Q)$ procedure, as summarized above, offers considerable savings in the computational effort compared to its CCSDT parent. Indeed, the computational times and walker populations characterizing the early stages of CIQMC propagations, which are sufficient to produce enough information for the subsequent $CC(P;Q)$ calculations to recover the target CCSDT energetics to within fractions of a millihartree, are very small compared to the converged CIQMC runs. Next, the $CC(P)$ calculations using small fractions of the triply excited determinants captured in the early stages of the CIQMC propagations are much faster than the parent CCSDT computations using all triples. Finally, the computational times required to determine corrections $\delta(P;Q)$ due to the remaining T_3 correlations not captured by the preceding $CC(P)$ runs, which scale no worse than $\sim 2n_o^3n_u^4$, are much less than the $n_o^3n_u^5$ timings associated with full CCSDT iterations.

Another interesting feature of the semi-stochastic $CC(P;Q)$ algorithm, as defined by the above steps 1–5, is a systematic behavior of the $E^{(P+Q)}$ energies as τ varies from 0 to ∞ . Indeed, the initial, $\tau = 0$, $CC(P;Q)$ energy, where the P space is spanned by all singly and doubly excited determinants and the Q space consists of all triples, is identical to that obtained using the CR-CC(2,3) correction to CCSD. On the other hand, when $\tau = \infty$, so that the P space is spanned by all singly, doubly, and triply excited determinants and the Q space is empty, the $CC(P;Q)$ energy $E^{(P+Q)}$ becomes equivalent to its CCSDT parent. Thus, the CIQMC propagation time τ can be regarded as a continuation parameter connecting the approximate treatment of T_3 clusters, represented by CR-CC(2,3), with their complete description offered by full CCSDT. As $\tau \rightarrow \infty$, the uncorrected $CC(P)$ energies $E^{(P)}$ converge to their CCSDT counterparts too, but, as shown in Refs. 95–97, and as illustrated via our calculations of the singlet–triplet gaps discussed in Section III, the convergence toward CCSDT is in this case substantially slower, since the initial, $\tau = 0$, $CC(P)$ energy is equivalent to that of CCSD, where $T_3 = 0$. The main role of corrections $\delta(P;Q)$ in the context of the semi-stochastic $CC(P;Q)$ algorithm considered in this study is to accelerate convergence of the underlying $CC(P)$ energies toward the desired CCSDT limit.

III. RESULTS

As explained in the Introduction, in order to assess the performance of our semi-stochastic, CIQMC-driven, $CC(P;Q)$ methodology in converging the full CCSDT data for the singlet–triplet gaps and the corresponding singlet- and triplet-state energies of biradical systems, we applied it to methylene, $(\text{HFH})^-$, cyclobutadiene, cyclopentadienyl cation, and trimethylenemethane. Following our earlier studies of the singlet–triplet gaps in the same systems using the deterministic $CC(P;Q)$ ⁵² and DEA/DIP-EOMCC^{123,124,135,136} approaches, we used the aug-cc-pVTZ basis set^{140,141} for methylene, the 6-31G(d,p) basis^{142,143} for the $(\text{HFH})^-$ ion, and the cc-pVDZ basis set¹⁴⁰ for cyclobutadiene, cyclopentadienyl cation, and trimethylenemethane. In the case of methylene and trimethylenemethane, we focused on the ability of the semi-stochastic $CC(P;Q)$ algorithm to converge the adiabatic ΔE_{S-T} data obtained with CCSDT. When executing the semi-stochastic $CC(P;Q)$ calculations for $(\text{HFH})^-$, cyclobutadiene, and cyclopentadienyl cation, we focused on recovering the CCSDT values of the vertical singlet–triplet gaps. Throughout this work, we define ΔE_{S-T} as $E_S - E_T$, where E_S and E_T are the electronic energies of the corresponding singlet and triplet states, i.e., the positive ΔE_{S-T} value implies that triplet is lower in energy.

All of the CC calculations reported in this article were performed using our group’s standalone codes, interfaced with the RHF, ROHF, and integral transform-

mation routines in the GAMESS package,^{144,145} which were originally developed in Refs. 50–53 and extended to the stochastically generated P spaces for the use in $CC(P)$ and $CC(P;Q)$ computations in Refs. 95–98. The i -FCIQMC [methylene, $(\text{HFH})^-$, and cyclobutadiene] and i -CISDTQ-MC (cyclopentadienyl cation and trimethylenemethane) calculations, needed to generate the lists of triples for the semi-stochastic $CC(P)$ and $CC(P;Q)$ runs, were carried out with the HANDE software.^{146,147} Each of the i -FCIQMC and i -CISDTQ-MC propagations was initiated by placing 1500 walkers on the relevant reference determinant. The CIQMC time step $\delta\tau$ and the initiator parameter n_a were set at 0.0001 a.u. and 3, respectively. In all post-Hartree–Fock calculations, the core MOs correlating with the 1s orbitals of the C and F atoms were kept frozen. If the true point group of the biradical system of interest was not Abelian, we used its largest Abelian subgroup, since our CC codes interfaced with GAMESS and the CIQMC routines in HANDE cannot handle non-Abelian symmetries.

A. Methylene

We begin the discussion of our results by analyzing the performance of the semi-stochastic $CC(P;Q)$ approach in converging the CCSDT energies of the ground (X^3B_1) and first-excited (A^1A_1) states of the methylene/aug-cc-pVTZ system and the adiabatic gap between them. The C_{2v} -symmetric geometries of CH_2 in the two states, optimized using FCI and the [5s3p/3s] triple zeta basis set of Dunning¹⁴⁸ augmented with two sets of polarization functions (TZ2P), were taken from Ref. 149. The electronically nondegenerate triplet ground state has a predominantly SR nature dominated by the $(1a_1)^2(2a_1)^2(1b_2)^2(3a_1)^1(1b_1)^1$ configuration, whereas the first-excited singlet state exhibits a significant MR character requiring a linear combination of the $(1a_1)^2(2a_1)^2(1b_2)^2(3a_1)^2$ and doubly excited $(1a_1)^2(2a_1)^2(1b_2)^2(1b_1)^2$ closed-shell determinants for a proper zeroth-order description. Because of these fundamentally different characteristics of the X^3B_1 and A^1A_1 states, a well-balanced and accurate treatment of dynamical and nondynamical correlation effects is the key to a reliable description of the singlet–triplet gap in methylene. It is, therefore, unsurprising that one usually resorts to methods of the MRCI^{149–154} or MRCC^{155–158} type, or to the high-level SRCC theories that account for higher-than-doubly excited clusters in an iterative manner, such as full CCSDT used in Refs. 23 and 52, to accomplish this goal (for other examples of high-level *ab initio* calculations for the X^3B_1 and A^1A_1 states of methylene, see Refs. 123, 135, 136, and 159 and references therein). The CCSDT results for the adiabatic singlet–triplet gap in methylene, which are of interest in the present study, are indeed very accurate. As shown, for example, in Ref. 52, the difference between the adiabatic ΔE_{S-T} value obtained in the CCSDT/TZ2P calculations

and the corresponding FCI result of 11.14 kcal/mol¹⁴⁹ is only 0.11 kcal/mol or 38 cm^{-1} . As demonstrated in Ref. 52 as well, the purely electronic $A^1A_1 - X^3B_1$ separation resulting from the CCSDT computations using the aug-cc-pVTZ basis employed in this work is only about 0.15 kcal/mol ($\sim 50 \text{ cm}^{-1}$) higher than the experimentally derived value of 9.37 kcal/mol reported in Ref. 156, obtained by correcting the vibrationless adiabatic singlet–triplet gap determined in Ref. 160 for the relativistic and nonadiabatic (Born–Oppenheimer diagonal correction) effects estimated in Refs. 161 and 162, respectively. It is, therefore, interesting to examine if the semi-stochastic $CC(P;Q)$ approach advocated in this work is capable of reproducing the high-quality CCSDT/aug-cc-pVTZ data for the X^3B_1 and A^1A_1 states of methylene and the adiabatic separation between them.

The results of our FCIQMC-driven $CC(P;Q)$ calculations for the methylene/aug-cc-pVTZ system, reported as errors relative to the parent CCSDT data, and their $CC(P)$ counterparts are shown in Table I and Fig. 1. The reference determinants $|\Phi\rangle$ used to initiate the i -FCIQMC propagations and to carry out the $CC(P)$, $CC(P;Q)$, CCSD, CR-CC(2,3), and CCSDT calculations were the ROHF determinant in the case of the X^3B_1 state and the RHF determinant for the A^1A_1 state. The subsets of triply excited determinants needed to construct the P spaces used in the $CC(P)$ and $CC(P;Q)$ computations at various propagation times τ were the $S_z = 1$ triples of the B_1 symmetry captured during the i -FCIQMC run for the X^3B_1 state and the $S_z = 0$ triples of the A_1 symmetry captured during the analogous run for the A^1A_1 state. Following the semi-stochastic $CC(P;Q)$ algorithm described in Section II, the Q spaces needed to determine corrections $\delta(P;Q)$ were defined as the remaining triples not captured by i -FCIQMC.

Let us start our analysis by examining the $CC(P)$ and $CC(P;Q)$ data at $\tau = 0$, where the P spaces do not contain any triply excited determinants. As shown in Table I, the $CC(P)$ energies of the X^3B_1 and A^1A_1 states at $\tau = 0$, which are equivalent to those obtained using conventional CCSD, are above their CCSDT [i.e., $\tau = \infty$ $CC(P)$] counterparts by 4.187 and 5.918 millihartree, respectively. This translates into a 380 cm^{-1} or $\sim 11\%$ error in the adiabatic ΔE_{S-T} value when compared to the 3328 cm^{-1} singlet–triplet gap obtained with CCSDT. The situation improves when the $CC(P;Q)$ corrections $\delta(P;Q)$ due to T_3 correlation effects, calculated by placing all triply excited determinants in the respective Q spaces, are added to the $CC(P)$ energies. The $\tau = 0$ $CC(P;Q)$ or CR-CC(2,3) energy characterizing the X^3B_1 state is only 0.177 millihartree above the parent CCSDT value, which is an error reduction relative to CCSDT compared to the underlying $CC(P)$ result by a factor of ~ 24 . The $\delta(P;Q)$ correction improves the $\tau = 0$ $CC(P)$ energy of the more challenging A^1A_1 state as well, although the difference between the resulting CR-CC(2,3) energy and its CCSDT counterpart, of 0.656 millihartree, is almost 4 times larger than the analogous

difference obtained for the X^3B_1 state. As a result, the 105 cm^{-1} error relative to CCSDT characterizing the adiabatic $A^1A_1 - X^3B_1$ separation obtained in the $\tau = 0$ $CC(P;Q)$ or $CR-CC(2,3)$ calculations, while considerably smaller than the 380 cm^{-1} obtained in the underlying $CC(P)$ (i.e., CCSD) runs, leaves room for further improvements. One can improve the $CR-CC(2,3)$ energies of the X^3B_1 and A^1A_1 states and the gap between them by enriching the P spaces defining the $CC(P)$ calculations with the leading triply excited determinants identified using active orbitals and correcting the resulting CCSDt energies for the remaining T_3 correlations that have not been captured by CCSDt,⁵² but our objective here is to examine if one can accomplish the same, or improve the $CC(t;3)$ results reported in Ref. 52 even further, by turning to the more black-box semi-stochastic $CC(P;Q)$ methodology, in which the dominant triply excited determinants are identified with CIQMC.

The results in Table I and Fig. 1 show that when the $\tau = 0$ P spaces are augmented with the subsets of triply excited determinants captured in the i -FCIQMC runs at $\tau > 0$ and, following the $CC(P;Q)$ recipe, the resulting $CC(P)$ energies are corrected for the remaining T_3 correlations, the convergence of the total electronic energies of the X^3B_1 and A^1A_1 states and the adiabatic separation between them toward their CCSDT parents is rapid. We can see this already in the early stages of the i -FCIQMC propagations. For example, at $\tau = 0.8$ a.u., i.e., after only 8000 $\delta\tau = 0.0001$ a.u. MC iterations, the errors in the $CC(P;Q)$ energies of the X^3B_1 and A^1A_1 states and the corresponding ΔE_{S-T} value relative to CCSDT are 0.049 millihartree, 0.106 millihartree, and 13 cm^{-1} , respectively, substantially improving the $CR-CC(2,3)$ [i.e., $\tau = 0$ $CC(P;Q)$] calculations, which give 0.177 millihartree for the X^3B_1 state, 0.656 millihartree for the A^1A_1 state, and 105 cm^{-1} for ΔE_{S-T} . This confirms our expectation that the main source of errors in the $CR-CC(2,3)$ computations, especially in the case of the more MR A^1A_1 state, which is characterized by larger T_3 effects, is the use of the unrelaxed T_1 and T_2 amplitudes obtained with CCSD in constructing the correction due to triples. The FCIQMC-based $CC(P;Q)$ calculations at $\tau = 0.8$ a.u., which use as little as 16% of all triply excited determinants to define the P space for the X^3B_1 state and only 25% of all triples in the P space for the A^1A_1 state, are also more accurate than the $CC(t;3)$ computations reported in Ref. 52, which produced the 0.130 millihartree, 0.409 millihartree, and 61 cm^{-1} errors relative to CCSDT for the X^3B_1 and A^1A_1 energies and ΔE_{S-T} , respectively. This is all very promising, especially if we realize that the i -FCIQMC propagations used to generate the lists of triples for our semi-stochastic $CC(P;Q)$ runs, which work so well, are very far from convergence when $\tau = 0.8$ a.u. Indeed, as seen in Table S.1 of the supplementary material, the total numbers of walkers at 8000 $\delta\tau = 0.0001$ a.u. MC iterations, which are 132689 in the case of the X^3B_1 state and 165564 for the A^1A_1 state, represent tiny fractions, 2.17% and 1.11%, respec-

tively, of the total walker populations at $\tau = 20.0$ a.u., where we stopped our i -FCIQMC propagations.

As demonstrated in Table I and Fig. 1, the convergence of the energies of the X^3B_1 and A^1A_1 states and the gap between them resulting from the FCIQMC-driven $CC(P;Q)$ calculations remains fast at the larger propagation times τ as well. For example, if we allow i -FCIQMC to populate the respective P spaces with about 26–38% of all triples, which happens after 20000 $\delta\tau = 0.0001$ a.u. MC iterations, the $CC(P;Q)$ energies of the X^3B_1 and A^1A_1 states and the resulting singlet–triplet gap become practically indistinguishable from the parent CCSDT data, with errors in the total electronic energies and ΔE_{S-T} being only ~ 20 microhartree and 2 cm^{-1} , respectively. As shown in Table S.1 of the supplementary material, walker populations characterizing the X^3B_1 and A^1A_1 states produced by i -FCIQMC at 20000 $\delta\tau = 0.0001$ a.u. MC time steps are still very small compared to the total numbers of walkers at $\tau = 20.0$ a.u., where we terminated our i -FCIQMC propagations (4.11% for the X^3B_1 state and 2.17% in the case of the A^1A_1 state). It is also interesting to note that the more MR A^1A_1 state requires a higher fraction of triply excited determinants in the P space than its SR X^3B_1 counterpart to achieve similar accuracy levels in the semi-stochastic $CC(P;Q)$ computations for both states. For example, the i -FCIQMC propagation has to capture about 25% of all triples, for the inclusion in the P space, if we are to reduce errors relative to CCSDT in the $CC(P;Q)$ calculations for the A^1A_1 state to ~ 0.1 millihartree. In the case of the X^3B_1 state, the analogous fraction of triples is about 10% (cf. Table I). This highlights the importance of balancing the SR triplet state with the more MR singlet state in obtaining accurate ΔE_{S-T} estimates, which is not a problem for the semi-stochastic $CC(P;Q)$ methodology because the underlying i -FCIQMC wave function sampling is very effective in identifying the dominant higher–than–doubly excited determinants, to be included in the relevant P spaces, and the $\delta(P;Q)$ corrections to the $CC(P)$ energies take care of the remaining correlation effects of interest.

Before concluding this subsection and discussing other molecular examples, we would like to comment on the effectiveness of the noniterative corrections $\delta(P;Q)$, adopted in the $CC(P;Q)$ formalism, in accelerating convergence of the underlying $CC(P)$ calculations toward CCSDT. The $CC(P)$ and $CC(P;Q)$ error curves shown in Fig. 1 illustrate this best. It is clear from this figure that the $CC(P;Q)$ energies of the X^3B_1 and A^1A_1 states [Fig. 1 (a) and (b)] and the corresponding ΔE_{S-T} values [Fig. 1 (c)] converge to the parent CCSDT data much faster than in the case of the uncorrected $CC(P)$ computations. One can see the same by inspecting the numerical data shown in Table I. In this context, it is worth commenting on the $CC(P)$ and $CC(P;Q)$ results obtained after 8000 MC iterations. In that case, the $CC(P;Q)$ calculations reduce the ~ 2.4 millihartree errors relative to CCSDT characterizing the $CC(P)$ en-

ergies of the X^3B_1 and A^1A_1 states to 0.1 millihartree or less, which is a desired behavior, but the $CC(P;Q)$ ΔE_{S-T} value is less accurate than that obtained with the uncorrected $CC(P)$. One should not read too much into this though. The fact that the $CC(P;Q)$ calculations at 8000 MC iterations increase the very small 3 cm^{-1} error obtained with $CC(P)$ to 13 cm^{-1} is a coincidence arising from the accidental cancellation of errors in the $CC(P)$ total electronic energies obtained at this particular propagation time. Indeed, when the later stages of the i -FCIQMC propagations are considered, the differences between the $CC(P)$ and CCSDT values of ΔE_{S-T} become increasingly negative, reaching -107 cm^{-1} at 50000 MC iterations, before eventually converging to the CCSDT limit, whereas the corresponding $CC(P;Q)$ results display a smooth behavior, rapidly approaching CCSDT. In particular, they reduce the relatively large negative error value obtained for ΔE_{S-T} in the $CC(P)$ calculations at 50000 MC iterations to a numerical 0 cm^{-1} . This highlights, once again, the ability of the $CC(P;Q)$ corrections $\delta(P;Q)$ to offer a well-balanced description of the lowest singlet and triplet states in methylene, in addition to improving the individual state energies.

B. (HFH)⁻

Our next example is the linear, $D_{\infty h}$ -symmetric, (HFH)⁻ anion, a prototype magnetic system in which unpaired spins of terminal hydrogen atoms couple to singlet and triplet states via a polarizable diamagnetic bridge of F⁻.¹¹⁴ The energies of the lowest two electronic states of the (HFH)⁻ system, including the singlet ground state $X^1\Sigma_g^+$ and the first-excited triplet state $A^3\Sigma_u^+$, and the vertical gap between them, which is proportional to the magnetic exchange coupling constant J and which should approach zero as both H-F bonds are stretched to infinity, were used in the past to test various quantum chemistry approaches.^{52,53,57,58,114,135,136,163,164} Among them were methods developed in our group, including CR-CC(2,3),^{57,58} CR-CC(2,4),⁵³ the DIP-EOMCC approaches with full and active-space treatments of 4h2p correlations of top of CCSD,^{135,136} and the active-orbital-based CC(t;3), CC(t,q;3), and CC(t,q;3,4) hierarchy.^{52,53} Here, we test the alternative to CC(t;3) offered by the semi-stochastic, FCIQMC-driven, $CC(P;Q)$ algorithm aimed at the CCSDT energetics. As in our previous studies,^{52,53,57,58,135,136} we used the 6-31G(d,p) basis set and several stretches of both H-F bonds, including $R_{H-F} = 1.50, 1.75, 2.00, 2.50,$ and 4.00 \AA , where R_{H-F} is the distance between the hydrogen and fluorine nuclei.

An accurate computation of the singlet-triplet gap in the (HFH)⁻ system is complicated by the fact that, unlike the $A^3\Sigma_u^+$ state, which is weakly correlated and well represented by a single ROHF determinant, its ground-state counterpart $X^1\Sigma_g^+$ displays a substantial MR character that includes a significant contribution from the doubly excited (HOMO)² \rightarrow (LUMO)² determinant, in

addition to the RHF configuration. The MR character of the $X^1\Sigma_g^+$ state, which is already noticeable at shorter H-F separations and which substantially strengthens as R_{H-F} increases, can be illustrated by the ratio of the FCI expansion coefficients at the (HOMO)² \rightarrow (LUMO)² and RHF determinants or the equivalent T_2 cluster amplitude extracted from FCI, which increases, in absolute value, from 0.38 at $R_{H-F} = 1.50 \text{ \AA}$ to 1.17 at $R_{H-F} = 4.00 \text{ \AA}$, when the 6-31G(d,p) basis is employed^{57,58} (the HOMO and LUMO have different symmetries, σ_g and σ_u , respectively, so that the HOMO \rightarrow LUMO T_1 amplitude is zero). As a result of all this, it is difficult to balance the lowest two states of the (HFH)⁻ system in a single quantum chemistry calculation, especially when the SRCC framework using the RHF reference determinant for the $X^1\Sigma_g^+$ state and the ROHF reference for the $A^3\Sigma_u^+$ state is employed. Indeed, as shown in Refs. 52, 57, and 58, the differences between the energies obtained in the CCSD/6-31G(d,p) computations and their FCI counterparts at $R_{H-F} = 1.50 \text{ \AA}$ are 12.674 millihartree for the $X^1\Sigma_g^+$ state and only 2.628 millihartree when the $A^3\Sigma_u^+$ state is considered. The analogous differences at $R_{H-F} = 2.00 \text{ \AA}$ are 19.398 and 2.068 millihartree, respectively. The observed large discrepancies between the errors in the CCSD energies for the $X^1\Sigma_g^+$ and $A^3\Sigma_u^+$ states translate into a poor description of the singlet-triplet gaps. One can see this by comparing the ΔE_{S-T} values resulting from the RHF/ROHF-based CCSD/6-31G(d,p) computations at $R_{H-F} = 1.50, 1.75, 2.00, 2.50,$ and 4.00 \AA with the corresponding FCI data. CCSD/6-31G(d,p) gives $-7320, -1838, 1656, 3605,$ and 230 cm^{-1} , respectively, as opposed to $-9525, -4911, -2147, -277,$ and 0 cm^{-1} obtained with FCI.^{52,57,58} If we are to improve the CCSD results within the SRCC framework, we must turn to higher-level theories, such as the CCSDT approach that interests us in this study,^{52,53,163} CCSDTQ,⁵³ or the DIP-EOMCC methodology, especially after incorporating 4h2p correlations.^{135,136} The CCSDT method is indeed very accurate, reducing the 2205, 3073, 3804, 3882, and 230 cm^{-1} errors relative to FCI in the ΔE_{S-T} values obtained with CCSD/6-31G(d,p) at $R_{H-F} = 1.50, 1.75, 2.00, 2.50,$ and 4.00 \AA to 198, 270, 341, 420, and 58 cm^{-1} , respectively.^{52,53,163} It also greatly improves the total electronic energies. Indeed, the differences between the CCSDT and FCI energies of the $X^1\Sigma_g^+$ and $A^3\Sigma_u^+$ states in the entire $R_{H-F} = 1.50 - 4.00 \text{ \AA}$ region obtained using the 6-31G(d,p) basis set do not exceed 2.276 and 0.389 millihartree, respectively.^{52,53} The analogous differences between the CCSD and FCI energies are as large as 20.546 millihartree for the former state and 2.628 millihartree when the latter state is considered. One can reduce the remaining small errors in the CCSDT results even further or practically eliminate them by using CCSDTQ⁵³ or the DIP-EOMCC approaches with 4h2p contributions,^{135,136} but the objective of this study is to assess the performance of our semi-stochastic $CC(P;Q)$ methodology in converging the CCSDT data.

The results of our FCIQMC-driven $CC(P;Q)/6-31G(d,p)$ computations for the $X^1\Sigma_g^+$ and $A^3\Sigma_u^+$ states of the linear $(HFH)^-$ system at the H-F distances $R_{H-F} = 1.50, 1.75, 2.00, 2.50,$ and 4.00 Å and the corresponding ΔE_{S-T} values, along with the underlying $CC(P)$ data, are reported in Tables II–IV and Fig. 2. In all of our $CC(P)$ and $CC(P;Q)$ computations and the underlying i -FCIQMC runs for the $D_{\infty h}$ -symmetric $(HFH)^-$ system, we used the D_{2h} Abelian subgroup of $D_{\infty h}$. In particular, the i -FCIQMC calculations for the $X^1\Sigma_g^+$ and $A^3\Sigma_u^+$ states were set up to converge the lowest-energy states of the $^1A_g(D_{2h})$ and $^3B_{1u}(D_{2h})$ symmetries. As a result, the subsets of triply excited determinants used to construct the P spaces for the subsequent $CC(P)$ and $CC(P;Q)$ computations for the $X^1\Sigma_g^+$ state at the various R_{H-F} and τ values considered in this work were defined as the $S_z = 0$ triples of the $A_g(D_{2h})$ symmetry captured in the underlying i -FCIQMC propagations. Similarly, the subsets of triply excited determinants used to design the P spaces for the $CC(P)$ and $CC(P;Q)$ calculations for the $A^3\Sigma_u^+$ state were the $S_z = 1$ triples of the $B_{1u}(D_{2h})$ symmetry extracted from i -FCIQMC. In analogy to all other $CC(P;Q)$ computations performed in this work, the Q spaces used to determine the $\delta(P;Q)$ corrections to the $CC(P)$ energies were defined as the remaining triples not captured by the respective i -FCIQMC runs.

As shown in Table II, and in line with our earlier $CC(P;Q)$ work⁵² and the above remarks, the $CC(P)$ energies of the $X^1\Sigma_g^+$ state of $(HFH)^-$ obtained at $\tau = 0$, which are identical to those resulting from the conventional CCSD calculations reported in Refs. 52, 57, and 58, are characterized by large errors relative to their $\tau = \infty$, i.e., CCSDT, parents. Indeed, the differences between the $\tau = 0$ and $\tau = \infty$ $CC(P)$ energies for the $X^1\Sigma_g^+$ state increase from 11.412 millihartree at $R_{H-F} = 1.50$ Å to more than 17 millihartree at $R_{H-F} = 2.00$ and 2.50 Å. These differences become smaller at large H-F separations, represented in our calculations by $R_{H-F} = 4.00$ Å, where the $D_{\infty h}$ -symmetric $(HFH)^-$ system is essentially dissociated into the stretched hydrogen molecule, which has only two electrons, so that CCSD becomes exact, and the closed-shell fluoride ion, which has the electronic structure of the neon atom and which is characterized by small T_n correlations with $n > 2$, but they remain large when the R_{H-F} values are smaller. This should be contrasted with the small, ~ 1 –2 millihartree, differences between the $\tau = 0$ and $\tau = \infty$ $CC(P)$ energies obtained at all values of R_{H-F} for the predominantly SR $A^3\Sigma_u^+$ state (see Table III). As already alluded to above, and as shown in Table IV, this imbalance in the description of the $X^1\Sigma_g^+$ and $A^3\Sigma_u^+$ states by the CCSD, i.e., $\tau = 0$ $CC(P)$, calculations gives rise to large errors in the resulting ΔE_{S-T} values relative to their $\tau = \infty$ (CCSDT) counterparts, which range from 2007 cm^{-1} to 3462 cm^{-1} in the $R_{H-F} = 1.50$ –2.50 Å region. Once again, these

errors become small at large H-F separations, such as $R_{H-F} = 4.00$ Å used in this work, where $(HFH)^-$ is more or less equivalent to the stretched H_2 and F^- , resulting in the nearly degenerate singlet and triplet states and the 172 cm^{-1} difference between the $\tau = 0$ and $\tau = \infty$ $CC(P)$ values of ΔE_{S-T} , but at shorter H-F distances they are large and comparable to or even larger than the singlet–triplet gap values provided by CCSDT or FCI.

The situation dramatically changes, when the $\tau = 0$ $CC(P)$ or CCSD energies are corrected for T_3 correlations with the help of the noniterative correction $\delta(P;Q)$, as in the $\tau = 0$ $CC(P;Q)$ calculations, which are equivalent to the purely deterministic CR-CC(2,3) runs reported in Refs. 52, 53, 57, and 58. As shown in Tables II–IV, the $\tau = 0$ $CC(P;Q)$, i.e., CR-CC(2,3), energies of the $X^1\Sigma_g^+$ and $A^3\Sigma_u^+$ states at the various H-F distances considered in this study and the gaps between them are substantially more accurate than their uncorrected $CC(P)$ (i.e., CCSD) counterparts. For example, the CR-CC(2,3) approach reduces the large, more than 17 millihartree, errors in the CCSD energies of the $X^1\Sigma_g^+$ state relative to their CCSDT [$\tau = \infty$ $CC(P)$ or $CC(P;Q)$] parents at $R_{H-F} = 2.00$ and 2.50 Å to ~ 1 –3 millihartree. We see similarly significant improvements in the CCSD energies of the $X^1\Sigma_g^+$ state by CR-CC(2,3) at other H-F distances, even at the “easiest” $R_{H-F} = 4.00$ Å value, where the triples correction $\delta(P;Q)$ is capable of reducing the already small, 1.907 millihartree, difference between the CCSD and CCSDT energies to the much smaller (in absolute value) 0.291 millihartree (see Table II). Consistent with our earlier studies,^{52,53,57,58} the CR-CC(2,3) method performs even better when the weakly correlated $A^3\Sigma_u^+$ state is examined, reducing the ~ 1 –2 millihartree errors in the underlying CCSD energetics relative to our CCSDT target to about 0.2 millihartree (see Table III). As a result of all of these accuracy improvements, the singlet–triplet gap values obtained using CR-CC(2,3) are much closer to their CCSDT parents than their CCSD counterparts, reducing the 2007, 2803, 3462, 3462, and 172 cm^{-1} errors relative to CCSDT obtained with CCSD at $R_{H-F} = 1.50, 1.75, 2.00, 2.50,$ and 4.00 Å, respectively, by factors ranging from 6 at $R_{H-F} = 2.50$ Å to 72 at $R_{H-F} = 1.50$ Å, but, as shown in Table IV [see, also, Ref. 52, where one can find a comparison of the CCSD, CR-CC(2,3), and CCSDT ΔE_{S-T} data for additional H-F distances], the differences on the order of (-600) – (-300) cm^{-1} between the CR-CC(2,3) and CCSDT singlet–triplet separations in the intermediate $R_{H-F} = 2.00$ –3.00 Å region remain. The question arises if one can refine the CR-CC(2,3) results by enriching the P spaces used in the $CC(P;Q)$ calculations, which in CR-CC(2,3) consist of only singles and doubles, with the subsets of triply excited determinants identified by i -FCIQMC propagations.

As shown in Tables II–IV and Fig. 2, once the leading triply excited determinants, captured using i -FCIQMC at $\tau > 0$, are included in the respective P spaces and the

$\delta(P;Q)$ corrections due to the remaining T_3 correlations are added to the energies obtained in the $CC(P)$ calculations, the resulting $CC(P;Q)$ values of the $X^1\Sigma_g^+$ and $A^3\Sigma_u^+$ energies and vertical gaps between them display very fast convergence toward their CCSDT counterparts. This is already observed when the i -FCIQMC propagation times are short, engaging tiny walker populations that are orders of magnitude smaller than those required to converge the i -FCIQMC runs, and the fractions of the triply excited determinants captured by i -FCIQMC are small. For example, after as few as 2000 $\delta\tau = 0.0001$ a.u. MC iterations, where τ is only 0.2 a.u. and where, as shown in Table S.2 of the supplementary material, the total walker populations characterizing the underlying i -FCIQMC runs are 0.01–0.11% of the respective numbers of walkers at $\tau = 20.0$ a.u. [the termination time for our i -FCIQMC propagations for $(\text{HFH})^-$], the differences between the $CC(P;Q)$ and CCSDT energies obtained for the strongly correlated $X^1\Sigma_g^+$ state are -0.035 millihartree for $R_{\text{H-F}} = 1.50$ Å, -0.056 millihartree for $R_{\text{H-F}} = 1.75$ Å, -0.110 millihartree for $R_{\text{H-F}} = 2.00$ Å, -0.583 millihartree for $R_{\text{H-F}} = 2.50$ Å, and -0.025 millihartree for $R_{\text{H-F}} = 4.00$ Å. In spite of using only about 10–30% of all triply excited determinants in the underlying P spaces, the FCIQMC-based $CC(P;Q)$ energies of the $X^1\Sigma_g^+$ state obtained after 2000 MC iterations reduce the errors relative to CCSDT characterizing the CR-CC(2,3) [i.e., $\tau = 0$ $CC(P;Q)$] computations in the $R_{\text{H-F}} = 1.50$ – 4.00 Å region by factors ranging from 5 to 13 (see Table II). In fact, with an exception of $R_{\text{H-F}} = 2.00$ and 2.50 Å, they are much more accurate than the results produced by the purely deterministic $CC(t;3)$ analog of the semi-stochastic $CC(P;Q)$ methodology, reported in Refs. 52 and 53. One can observe even more dramatic improvements over CR-CC(2,3) offered by the FCIQMC-driven $CC(P;Q)$ approach, when the propagation time τ increases. For example, after 4000 MC iterations, where the i -FCIQMC propagations are still far from being converged (cf. the total walker populations used by our i -FCIQMC runs relative to the termination time $\tau = 20.0$ a.u. in Table S.2 of the supplementary material) and the fractions of triples included in the stochastically determined P spaces, which range from 12% at $R_{\text{H-F}} = 4.00$ Å to 56% at $R_{\text{H-F}} = 1.50$ Å, remain relatively small, the differences between the $CC(P;Q)$ and CCSDT energies obtained for the $X^1\Sigma_g^+$ state at $R_{\text{H-F}} = 1.50, 1.75, 2.00, 2.50,$ and 4.00 Å are $-28, -9, -17, -50,$ and -4 microhartree, respectively, reducing the errors relative to CCSDT that characterize the corresponding CR-CC(2,3) calculations by factors ranging from 12 to 86 [2 to 61 when compared to the $CC(t;3)$ results reported in Refs. 52 and 53]. As shown in Table III, the performance of the FCIQMC-driven $CC(P;Q)$ approach becomes even more impressive when the $A^3\Sigma_u^+$ state, which has a SR character, is examined. After 2000 $\delta\tau = 0.0001$ a.u. MC time steps, the errors in

the $CC(P;Q)$ energies relative to their CCSDT parents obtained for the $A^3\Sigma_u^+$ state at $R_{\text{H-F}} = 1.50, 1.75, 2.00, 2.50,$ and 4.00 Å are only $-40, -24, -38, -29,$ and -14 microhartree, respectively. After 4000 MC iterations, they become $-10, -10, -12, -9,$ and -2 microhartree, respectively. Once again, these are considerable improvements compared to CR-CC(2,3) and $CC(t;3)$ that both give errors on the order of -0.2 millihartree,^{52,53} especially if we realize that the fractions of triples captured by the i -FCIQMC runs after 2000 and 4000 MC iterations are relatively small (5–28% and 5–49%, respectively) and, as shown in Table S.2 of the supplementary material, the corresponding numbers of walkers represent only about 1–2% of the total numbers of walkers at $\tau = 20.0$ a.u., where we stopped our i -FCIQMC propagations.

As a consequence of the small errors in the $CC(P;Q)$ total energies characterizing the $X^1\Sigma_g^+$ and $A^3\Sigma_u^+$ states in the early stages of the i -FCIQMC propagations, the resulting singlet–triplet gap values are very accurate as well. This is demonstrated in Table IV, where one can see that after 2000 $\delta\tau = 0.0001$ a.u. MC iterations, which is, as already explained, a very short propagation time engaging tiny walker populations and small fractions of triples, most of the differences between the $CC(P;Q)$ and CCSDT $\Delta E_{\text{S-T}}$ values in the $R_{\text{H-F}} = 1.50$ – 4.00 Å region are on the order of a few reciprocal centimeter. The only exception is the semi-stochastic $CC(P;Q)$ run at $R_{\text{H-F}} = 2.50$ Å, where the -122 cm^{-1} error relative to CCSDT characterizing the singlet–triplet gap obtained after 2000 MC time steps, while representing a five-fold error reduction compared to CR-CC(2,3), is comparable, in magnitude, to the CCSDT value of $\Delta E_{\text{S-T}}$. This happens because the $CC(P;Q)$ energy of the strongly correlated $X^1\Sigma_g^+$ state obtained after 2000 MC iterations at $R_{\text{H-F}} = 2.50$ Å differs from its CCSDT parent by -0.583 millihartree, whereas the analogous difference between the $CC(P;Q)$ and CCSDT energies for its weakly correlated $A^3\Sigma_u^+$ companion is only -29 microhartree. This is not a problem though, since by running i -FCIQMC a little longer and capturing about 20% of all triply excited determinants in the relevant P spaces, as is the case when 4000 $\delta\tau = 0.0001$ a.u. MC time steps are considered, one reduces the differences between the $CC(P;Q)$ and CCSDT energies of the $X^1\Sigma_g^+$ and $A^3\Sigma_u^+$ states to -50 and -9 microhartree, respectively (cf. Tables II and III), so that the 122 cm^{-1} unsigned error in the $CC(P;Q)$ value of $\Delta E_{\text{S-T}}$ relative to CCSDT obtained after 2000 MC iterations decreases to less than 10 cm^{-1} . This is yet another illustration of the ability of the semi-stochastic $CC(P;Q)$ methodology pursued in this work to balance the more MR singlet and weakly correlated triplet states of biradical systems in a single computation at the fraction of the cost of the parent high-level CC calculations. As shown in Table IV, at $\tau = 0.4$ a.u., where the i -FCIQMC propagations are still far from being converged, the FCIQMC-driven $CC(P;Q)$ calculations recover the CCSDT values of the singlet–triplet gaps in $(\text{HFH})^-$ at

all H–F distances considered in this study to within a few reciprocal centimeter, reaching a 1–2 cm^{-1} or better accuracy after 6000 MC iterations.

Last, but not least, the results reported in Tables II–IV and Fig. 2 also demonstrate the remarkable efficiency of the $\delta(P;Q)$ corrections in accelerating the convergence of the $CC(P)$ energies of the $X^1\Sigma_g^+$ and $A^3\Sigma_u^+$ states and the vertical gaps between them toward CCSDT, independent of the H–F distance considered. Let us, for example, compare the uncorrected $CC(P)$ and corrected $CC(P;Q)$ energies of the $X^1\Sigma_g^+$ and $A^3\Sigma_u^+$ states of $(\text{HFH})^-$ at the five H–F separations considered in this work obtained after 2000 MC iterations. In the case of the former, more MR, state, the $CC(P;Q)$ corrections $\delta(P;Q)$ reduce the positive 2.601, 3.998, 3.511, 6.586, and 0.412 millihartree errors relative to CCSDT resulting from the $CC(P)$ computations at $R_{\text{H-F}} = 1.50, 1.75, 2.00, 2.50,$ and 4.00 Å to the much smaller negative error values of $-0.035, -0.056, -0.110, -0.583,$ and -0.025 millihartree, respectively. When the latter state, which is characterized by much weaker correlations, is considered, the $CC(P;Q)$ approach reduces the 0.995, 0.826, 0.834, 0.502, and 0.239 millihartree errors obtained with $CC(P)$ to $-40, -24, -38, -29,$ and -14 microhartree, respectively. It is interesting to notice that while the errors characterizing the $CC(P)$ calculations for the $A^3\Sigma_u^+$ state are generally much smaller than their $X^1\Sigma_g^+$ counterparts, and the two states have a substantially different character, the error reductions offered by the $CC(P;Q)$ corrections $\delta(P;Q)$, by at least one order of magnitude, apply to both states. As already alluded to above, and as shown in Table IV and Fig. 2 (e) and (f), where we examine the convergence of the $CC(P)$ and $CC(P;Q)$ $\Delta E_{\text{S-T}}$ values toward their CCSDT parents, the noniterative corrections $\delta(P;Q)$ are also very effective in improving the balance in the description of the $X^1\Sigma_g^+$ and $A^3\Sigma_u^+$ states by the $CC(P)$ approach and smoothing the convergence of the resulting singlet–triplet gaps toward their CCSDT limits. This can be illustrated by comparing the behavior of the error values relative to CCSDT characterizing the $CC(P)$ calculations of $\Delta E_{\text{S-T}}$ at $R_{\text{H-F}} = 2.00$ Å with their $CC(P;Q)$ counterparts, shown in Table IV. In the former case, the 3462 cm^{-1} error at $\tau = 0$ decreases, in absolute value, to 8 cm^{-1} at $\tau = 0.8$ a.u. (8000 MC iterations), to increase to 17 cm^{-1} at $\tau = 2.0$ a.u. (20000 MC iterations), to decrease again to a numerical 0 cm^{-1} at $\tau = 20.0$ a.u. (200000 MC iterations). Once the $CC(P)$ energies of the $X^1\Sigma_g^+$ and $A^3\Sigma_u^+$ states are corrected using the $\delta(P;Q)$ corrections, the unsigned errors in the resulting $CC(P;Q)$ values of $\Delta E_{\text{S-T}}$ relative to their CCSDT parent monotonically and rapidly decrease, from 282 cm^{-1} at $\tau = 0$ to a numerical 0 cm^{-1} at $\tau \geq 0.8$ a.u. It is clear from Tables II–IV and Fig. 2 that while both the $CC(P)$ and $CC(P;Q)$ energies converge to the parent CCSDT limit, the latter energies and the gaps between them converge to CCSDT a lot faster.

C. Cyclobutadiene and cyclopentadienyl cation

We now proceed to the examination of the performance of the semi-stochastic $CC(P;Q)$ algorithm in calculations involving medium-sized organic biradicals, starting from two prototypical anti-aromatic systems, cyclobutadiene and cyclopentadienyl cation, both described using the cc-pVDZ basis set. As in the rest of the present study, we are mainly interested in how efficient the CIQMC-driven $CC(P;Q)$ methodology is in recovering the CCSDT energies of the lowest singlet and triplet states and gaps between them. In the case of cyclobutadiene and cyclopentadienyl cation discussed in this subsection, we focus on examining vertical singlet–triplet gaps.

We begin with the FCIQMC-driven $CC(P;Q)$ calculations for cyclobutadiene, in which we adopted the D_{4h} -symmetric geometry that represents the transition state for the automerization of cyclobutadiene proceeding on the lowest singlet potential, optimized with the MR average-quadratic CC (MR-AQCC) approach^{165,166} using the cc-pVDZ basis in Ref. 167. We employed this geometry for two reasons. One of them is the fact that we used the same geometry in our earlier CIQMC- and CCMC-based,^{95,97} CIPSI-driven,¹⁰² and active-orbital-based⁵¹ $CC(P;Q)$ calculations for cyclobutadiene, when examining its automerization. Because of this, we could verify the correctness of our FCIQMC-driven $CC(P;Q)$ calculations for the lowest-energy singlet state, which is also the ground state of the system. Another is the observation that the D_{4h} -symmetric transition-state structure characterizing the automerization of cyclobutadiene is practically identical to the D_{4h} -symmetric minimum on the lowest triplet surface. Indeed, the MR-AQCC/cc-pVDZ C–C and C–H bond lengths defining the transition state on the ground-state singlet potential differ from those characterizing the triplet minimum optimized using unrestricted CCSD (UCCSD) in Ref. 118 by less than 0.009 and 0.001 Å, respectively.

At the D_{4h} -symmetric geometry used in our calculations, cyclobutadiene is characterized by the delocalization of four π electrons over four π MOs, which gives rise to the close-lying singlet and triplet states that require a highly accurate treatment of electron correlation effects if we are to obtain a well-balanced description of the two states and the small energy separation between them. One can understand this by examining the valence π network of the D_{4h} -symmetric cyclobutadiene species, which consists of the doubly occupied nondegenerate a_{2u} orbital, the doubly degenerate e_g level, in which each component MO is occupied by a single electron, and the nondegenerate b_{1u} orbital, which in the zeroth-order description of the lowest singlet and triplet states remains empty. The two valence electrons in the degenerate e_g shell can couple to a singlet or a triplet, resulting in the open-shell singlet ground state, X^1B_{1g} , which has a substantial MR character, and the first excited triplet state, A^3A_{2g} , which is predominantly SR in nature. In order to balance the substantial nondynamical correlation

effects, needed for an accurate description of the low-spin X^1B_{1g} state, with the dynamical correlations dominating its high-spin triplet A^3A_{2g} companion within a conventional, particle-conserving, SRCC framework and produce reliable ΔE_{S-T} values for cyclobutadiene, which could compete with the high-accuracy *ab initio* data reported in Refs. 118, 123, 124, 167–172, one has to consider robust treatments of the connected triply excited clusters, such as that offered by CCSDT.^{168,172} Indeed, full CCSDT, which is the target of this investigation, produces high-quality results for the lowest singlet and triplet states of the D_{4h} -symmetric cyclobutadiene system and the energy separation between them. For example, the ΔE_{S-T} value obtained in the CCSDT/cc-pVDZ calculations at the transition-state geometry used in the present study, of -4.8 kcal/mol, is practically identical to the results of the state-of-the-art DEA-EOMCC computations including the high-rank 4p2h correlations on top of CCSD, reported in Refs. 123 and 124, which give -5.0 kcal/mol when the cc-pVDZ basis set is employed (for similar recent observations regarding the reliability of full CCSDT in generating virtually exact singlet-triplet gap values for cyclobutadiene, see Ref. 172). It is, therefore, interesting to explore if the semi-stochastic $CC(P;Q)$ methodology investigated in this work is capable of converging the CCSDT results for the X^1B_{1g} and A^3A_{2g} states of cyclobutadiene and vertical gap between them out of the early stages of CIQMC propagations.

The results of our FCIQMC-driven $CC(P)$ and $CC(P;Q)$ computations for cyclobutadiene are summarized in Table V and Fig. 3. In all of our calculations, starting with the stochastic *i*-FCIQMC steps and ending with the deterministic $CC(P;Q)$ and CCSDT runs, we used the D_{2h} Abelian subgroup of the D_{4h} point group characterizing the cyclobutadiene’s geometry adopted in this work. Consequently, the *i*-FCIQMC propagations for the X^1B_{1g} and A^3A_{2g} states were set up to converge the lowest states of the $^1A_g(D_{2h})$ and $^3B_{1g}(D_{2h})$ symmetries. Consistent with the $CC(P)$ and $CC(P;Q)$ runs that follow the *i*-FCIQMC steps and the accompanying CCSD, CR-CC(2,3), and CCSDT computations, the reference determinants used to initiate our *i*-FCIQMC propagations were the closed-shell, D_{2h} -adapted, RHF function obtained by placing two electrons on one of the e_g valence orbitals for the lowest-energy $^1A_g(D_{2h})$ state and the high-spin ROHF determinant, adapted to D_{2h} as well, for the lowest $^3B_{1g}(D_{2h})$ state. As a result, the lists of triply excited determinants extracted from the *i*-FCIQMC runs at the various propagation times $\tau > 0$, needed to define the P spaces for the $CC(P)$ and $CC(P;Q)$ computations, consisted of the $S_z = 0$ triples of the $A_g(D_{2h})$ symmetry for the X^1B_{1g} state and the $S_z = 1$ triples of the $B_{1g}(D_{2h})$ symmetry in the case of the A^3A_{2g} state. Given our interest in converging the CCSDT energetics, the Q spaces used to construct the $\delta(P;Q)$ corrections consisted of the remaining triply excited determinants, absent in the *i*-FCIQMC wave functions of the X^1B_{1g} and A^3A_{2g} states at a given τ .

The results shown in Table V and Fig. 3 display several similarities with the previously discussed methylene and $(\text{HFH})^-$ cases. One cannot, for example, obtain an accurate description of the more MR singlet ground state and the energy separation between the X^1B_{1g} and A^3A_{2g} states without incorporating the leading triply excited determinants in the P space. Indeed, when the P space consists of only singly and doubly excited determinants, as in the $\tau = 0$ $CC(P)$ (i.e., CCSD) and $CC(P;Q)$ [i.e., CR-CC(2,3)] calculations, one ends up with the enormous errors in the energies of the X^1B_{1g} state relative to their CCSDT parent, which are 47.979 millihartree in the former case and 14.636 millihartree when the latter computation is considered. The $\tau = 0$ $CC(P;Q)$ energy of the A^3A_{2g} state is a lot more accurate, reducing the large, 23.884 millihartree, error relative to CCSDT obtained in the underlying $CC(P)$ calculation to -60 microhartree, but this does not help too much. The corresponding CR-CC(2,3) triples correction to CCSD, which neglects the coupling of the low-order T_1 and T_2 clusters with their higher-order T_3 counterpart, is incapable of offering a balanced description of the X^1B_{1g} and A^3A_{2g} states, so that the resulting singlet-triplet gap is very poor. The 9.2 kcal/mol difference between the ΔE_{S-T} values obtained in the $\tau = 0$ $CC(P;Q)$ or CR-CC(2,3) and CCSDT calculations is so large that the $X^1B_{1g} - A^3A_{2g}$ separation predicted by CR-CC(2,3) has a wrong sign compared to its -4.8 kcal/mol CCSDT counterpart, while being nearly identical in magnitude. This difference becomes even larger when the uncorrected $\tau = 0$ $CC(P)$, meaning CCSD, calculations are considered (15.1 kcal/mol).

As shown in Table V and Fig. 3, the situation dramatically changes when the P spaces used in the $CC(P)$ and $CC(P;Q)$ calculations are enriched with the subsets of triply excited determinants captured by the *i*-FCIQMC propagations. The convergence of the $CC(P;Q)$ energies of the X^1B_{1g} and A^3A_{2g} states, especially the former ones, and the vertical separations between them is particularly impressive. For example, after as few as 6000 $\delta\tau = 0.0001$ a.u. MC time steps and *i*-FCIQMC capturing less than 30% of all triples in the P space, where, as demonstrated in Table S.3 of the supplementary material, the walker population characterizing the *i*-FCIQMC run for the X^1B_{1g} state is only 0.02% of the total number of walkers at $\tau = 8.0$ a.u. (the termination time for our *i*-FCIQMC propagations for cyclobutadiene), the $CC(P;Q)$ approach reduces the 14.636 millihartree difference between the CR-CC(2,3) and CCSDT energies of the strongly correlated singlet ground state to 2.223 millihartree. While the CR-CC(2,3) description of the A^3A_{2g} state, which has a largely SR character, is already excellent, the $CC(P;Q)$ calculation performed after 6000 MC iterations, which uses only 26% of triples in the P space and a tiny walker population that amounts to 0.04% of all walkers at $\tau = 8.0$ a.u. in the underlying *i*-FCIQMC propagation, improves it too, reducing the small, 60 microhartree, unsigned difference between the CR-CC(2,3) and CCSDT energies to an even smaller 51 microhartree.

As a consequence of the above improvements, especially for the X^1B_{1g} state, the error relative to CCSDT characterizing the ΔE_{S-T} value obtained in the FCIQMC-driven $CC(P;Q)$ calculations after 6000 $\delta\tau = 0.0001$ a.u. MC time steps, where the underlying *i*-FCIQMC propagations are still in their early stages, is only 1.4 kcal/mol, as opposed to 9.2 kcal/mol obtained at $\tau = 0$ with CR-CC(2,3). The resulting $X^1B_{1g} - A^3A_{2g}$ energy separation, of -3.4 kcal/mol, has not only the correct sign, but is also very close to the -4.8 kcal/mol value obtained with CCSDT. If we wait a little longer, by executing the extra 2000 MC iterations, so that the *i*-FCIQMC propagations can capture 34%–39% of all triply excited determinants, we can reduce the already small 2.223 millihartree, 51 microhartree, and 1.4 kcal/mol errors in the $CC(P;Q)$ energies of the X^1B_{1g} and A^3A_{2g} states and separation between them relative to CCSDT, obtained after 6000 MC time steps, to 0.835 millihartree, 31 microhartree, and 0.5 kcal/mol, respectively. It is clear from Table V and Fig. 3 that the convergence of the semi-stochastic $CC(P;Q)$ results for the lowest-energy singlet and triplet states of cyclobutadiene, especially the X^1B_{1g} energies and the $X^1B_{1g} - A^3A_{2g}$ gap values, which the $\tau = 0$ $CC(P;Q)$ or CR-CC(2,3) calculations describe poorly, toward CCSDT is very fast, even when the underlying *i*-FCIQMC propagations are far from convergence. It is also apparent from our calculations that the noniterative corrections $\delta(P;Q)$ play a significant role in accelerating convergence of the corresponding $CC(P)$ energetics toward CCSDT. As shown, for example, in Table V, the relatively large differences between the uncorrected $CC(P)$ energies of the X^1B_{1g} and A^3A_{2g} states and vertical gap between them obtained at $\tau = 0.8$ a.u., i.e., after 8000 $\delta\tau = 0.0001$ a.u. MC iterations, and the corresponding CCSDT data, which exceed 11 and 7 millihartree and 3 kcal/mol, respectively, are reduced to 0.835 millihartree, 31 microhartree, and 0.5 kcal/mol, when the $CC(P;Q)$ approach is employed. We can see similar improvements in the $CC(P)$ energies at other τ values.

Most of the observations regarding the performance of the semi-stochastic $CC(P;Q)$ methodology and its $CC(P)$ counterpart remain valid when the larger cyclopentadienyl cation, which is also the largest molecular system considered in our $CC(P)/CC(P;Q)$ work to date, is examined. Following our previous DEA-EOMCC studies of cyclopentadienyl cation,^{123,124} where we investigated the effect of high-order 4p2h correlations on its singlet–triplet gap, we used the D_{5h} -symmetric geometry corresponding to a minimum on the lowest triplet surface obtained in the UCCSD/cc-pVDZ optimization in Ref. 118. At this geometry, cyclopentadienyl cation is characterized by the delocalization of four π electrons over five π MOs, resulting in the doubly occupied nondegenerate a_2'' orbital, the doubly degenerate e_1'' shell, in which each component MO is occupied by a single electron, and the doubly degenerate e_2'' shell, which in the zeroth-order description of the lowest-energy singlet and triplet states remains empty. In analogy to the previously discussed cy-

clobutadiene system, the two electrons in the degenerate e_1'' MOs can couple to a singlet or triplet, but compared to cyclobutadiene, where the lowest-energy singlet state is also a ground state, the state ordering in cyclopentadienyl cation is reversed, so that the lowest triplet, designated as X^3A_2' , is the ground state and the lowest-energy singlet, denoted as A^1E_2' , is the first excited state. Similar to all other examples considered in this work, in order to obtain a well-balanced description of the X^3A_2' state, which has a SR character dominated by dynamical correlations, and its A^1E_2' companion, which is an open-shell singlet characterized by significant MR correlations, and obtain an accurate value of ΔE_{S-T} within a conventional SRCC framework, one must turn to higher-level theories that can offer a robust treatment of T_n clusters with $n > 2$. Otherwise, as shown in Ref. 118, and as confirmed in our calculations, the results can be very poor. For example, the $A^1E_2' - X^3A_2'$ separation in cyclopentadienyl cation resulting from the restricted CCSD calculations using the cc-pVDZ basis, which are equivalent to our $\tau = 0$ $CC(P)$ computations, is about 23 kcal/mol. This is in large disagreement with the most accurate *ab initio* calculations of the singlet–triplet gap in cyclopentadienyl cation performed to date using the DEA-EOMCC formalism including 3p1h as well as 4p2h correlations on top of the CCSD treatment of the underlying closed-shell core, which give about 14 kcal/mol when the cc-pVDZ basis set is employed^{123,124} (for the examples of other high-level SRCC and MRCC calculations of the singlet–triplet gap in cyclopentadienyl cation, see Ref. 118; Ref. 124 also provides the well-converged MR perturbation theory data, which agree with the state-of-the-art DEA-EOMCC computations reported in Refs. 123 and 124). The restricted CCSDT approach, which is the target SRCC method in this study, provides a much better description, reducing the approximately 9 kcal/mol error relative to the most accurate DEA-EOMCC calculations with up to 4p2h excitations reported in Refs. 123 and 124 obtained with restricted CCSD to less than 3 kcal/mol, when the cc-pVDZ basis set is employed. It would certainly be interesting to examine if the inclusion of higher-than–triply excited clusters, such as T_4 , could further improve the CCSDT description of the singlet–triplet gap in cyclopentadienyl cation, but in this work we focus on the ability of the semi-stochastic, CIQMC-based, $CC(P;Q)$ methodology to improve the CR-CC(2,3) ΔE_{S-T} values and converge the results of CCSDT computations. We hope to return to the topic of the role of T_4 clusters in describing the singlet–triplet gap in cyclopentadienyl cation in one of our future studies. It may be worth pointing out that the $A^1E_2' - X^3A_2'$ gap obtained in the restricted CCSDT/cc-pVDZ calculations, which give $\Delta E_{S-T} = 16.7$ kcal/mol, is in very good agreement with the 16.1 kcal/mol resulting from the DEA-EOMCC/cc-pVDZ computations truncated at 3p1h excitations.^{123,124}

The results of our CIQMC-driven $CC(P)$ and $CC(P;Q)$ computations for cyclopentadienyl cation are reported in Table VI and Fig. 4. As already alluded to

above, to reduce the computational costs of the CIQMC propagations preceding the $CC(P)$ and $CC(P;Q)$ steps, especially in the later stages of the CIQMC runs that are included in Table VI and Fig. 4 for the completeness of our presentation, we replaced the i -FCIQMC algorithm, which we exploited in our calculations for methylene, $(\text{HFH})^-$, and cyclobutadiene, by its truncated i -CISDTQ-MC counterpart. It has been established in Ref. 97 that the replacement of i -FCIQMC by i -CISDTQ-MC, when identifying the leading higher-than-doubly excited determinants for the inclusion in the P spaces used in the semi-stochastic $CC(P)$ and $CC(P;Q)$ runs, has virtually no effect on the rate at which these runs converge the parent SRCC energetics. In analogy to cyclobutadiene, all of our i -CISDTQ-MC, semi-stochastic $CC(P)$ and $CC(P;Q)$, and deterministic CCSD, CR-CC(2,3), and CCSDT computations utilized the largest Abelian subgroup of the D_{5h} point group characterizing the cyclopentadienyl cation’s structure examined in the present study, which is C_{2v} . This means that in setting up our calculations for the $X^3A'_2$ state, we treated it as the lowest state of the ${}^3B_2(C_{2v})$ symmetry, whereas the doubly degenerate $A^1E'_2$ state was represented by its ${}^1A_1(C_{2v})$ component. Similar to cyclobutadiene, and to remain consistent with the $CC(P)$, $CC(P;Q)$, and other SRCC runs for cyclopentadienyl cation carried out in this study, the reference determinant used to initiate the i -CISDTQ-MC propagation for the lowest-energy ${}^3B_2(C_{2v})$ state was the triplet ROHF determinant. In the case of the ${}^1A_1(C_{2v})$ component of the $A^1E'_2$ state, we used the RHF determinant obtained by pairing the two valence electrons in one of the e''_1 MOs to initiate the corresponding i -CISDTQ-MC run. Consistent with the above description, the subsets of triply excited determinants used to construct the P spaces for the semi-stochastic $CC(P)$ and $CC(P;Q)$ computations for the $X^3A'_2$ state were the $S_z = 1$ triples of the $B_2(C_{2v})$ symmetry captured by i -CISDTQ-MC. In the case of the $A^1E'_2$ state, represented, as explained above, by its ${}^1A_1(C_{2v})$ component, we used the $S_z = 0$ triples of the $A_1(C_{2v})$ symmetry identified by the i -CISDTQ-MC propagation set up to converge the lowest $A_1(C_{2v})$ state. As usual, the corresponding Q spaces were spanned by the remaining triply excited determinants that were not captured by the i -CISDTQ-MC runs when the lists of P -space triples were created.

Our calculations for cyclopentadienyl cation, summarized in Table VI and Fig. 4, demonstrate that the $CC(P;Q)$ energies of the $X^3A'_2$ and $A^1E'_2$ states and vertical gaps between them display fast convergence toward the respective CCSDT values with the propagation time τ . This is particularly apparent in the case of the $CC(P;Q)$ energies of the more MR $A^1E'_2$ state and the $A^1E'_2 - X^3A'_2$ separation, which cannot be accurately described if the underlying P spaces contain only singly and doubly excited determinants. Indeed, the CR-CC(2,3) energy of the $A^1E'_2$ state, which is equivalent to the $\tau = 0$ $CC(P;Q)$ value, is much more accurate than the result of the associated $CC(P)$ or CCSD calculation,

which produces the enormous error relative to CCSDT exceeding 38 millihartree, but the substantial, > 6 millihartree, difference with the CCSDT energy remains. The situation for the SR $X^3A'_2$ state, where the CR-CC(2,3) approach reduces the nearly 29 millihartree error relative to CCSDT obtained in the CCSD calculations to ~ 0.2 millihartree, is a lot better, but this does not help the resulting ΔE_{S-T} value, which differs from its CCSDT counterpart by almost 4 kcal/mol (almost a quarter of the CCSDT value of ΔE_{S-T}). The discrepancy between the errors in the CR-CC(2,3) energies of the $X^3A'_2$ and $A^1E'_2$ states is simply too large. Clearly, one needs to incorporate some triples in the corresponding P spaces, especially in the case of the more challenging $A^1E'_2$ state.

Once the $\tau = 0$ P spaces are augmented with the leading triply excited determinants identified by the i -CISDTQ-MC propagations and the noniterative corrections $\delta(P;Q)$ are added to the $CC(P)$ energies to estimate the effects of the remaining T_3 correlations, we observe smooth convergence of the resulting $CC(P;Q)$ energetics toward their respective CCSDT limits. This includes significant improvements in the poor description of the $A^1E'_2$ state and the $A^1E'_2 - X^3A'_2$ separation by CR-CC(2,3). As shown in Table VI, already after 10000 $\delta\tau = 0.0001$ a.u. MC time steps, where the i -CISDTQ-MC propagations are still in their infancy, capturing only 25–30% of all triples and using tiny walker populations, on the order of 0.1–0.2% of the total numbers of walkers at $\tau = 8.0$ a.u. (see Table S.4 of the supplementary material), the 6.245 millihartree and 3.8 kcal/mol errors in the energy of the $A^1E'_2$ state and the ΔE_{S-T} value relative to CCSDT obtained with CR-CC(2,3) reduce in the $CC(P;Q)$ calculations to 2.248 millihartree and 1.3 kcal/mol, respectively. By running i -CISDTQ-MC a little longer and capturing about 50–60% of all triples in the relevant P spaces, as is the case after 20000 MC iterations, where the walker populations compared to $\tau = 8.0$ a.u. are still tiny, the errors in the $CC(P;Q)$ values of the $A^1E'_2$ energy and ΔE_{S-T} relative to their CCSDT parents drop down by an order of magnitude compared to 10000 MC iterations, to 0.217 millihartree and 0.1 kcal/mol, respectively. Although the excellent description of the predominantly SR $X^3A'_2$ state by the CR-CC(2,3) approach hardly needs any improvement, the i -CISDTQ-MC-driven $CC(P;Q)$ calculations are helping here too, reducing the 0.245 millihartree difference between the CR-CC(2,3) and CCSDT energies to 0.108 millihartree after 10000 MC iterations (26 microhartree when the number of MC iterations is increased to 20000). As anticipated, the uncorrected $CC(P)$ energies of the $X^3A'_2$ and $A^1E'_2$ states converge to the respective CCSDT limits too, but they do it at a much slower pace than their $CC(P;Q)$ counterparts. A comparison of the results of the $CC(P)$ and $CC(P;Q)$ calculations for the $A^1E'_2 - X^3A'_2$ gap shown in Table VI and Fig. 4 (c) may create an impression as if the noniterative corrections $\delta(P;Q)$ offer very little, but this would be misleading. The relatively fast convergence of the

CC(P) values of ΔE_{S-T} toward their CCSDT parent in the early stages of the underlying i -CISDTQ-MC propagations, which compares well with that observed in the corresponding CC($P;Q$) computations, is a result of the fortuitous cancellation of large errors characterizing the CC(P) energies of the $X^3A'_2$ and $A^1E'_2$ states. Since no other system examined in this study displays similar error cancellations, and since costs of computing corrections $\delta(P;Q)$, which offer major error reductions in the individual CC(P) energies, while accelerating their convergence toward the SRCC target, are low, we recommend using the $\delta(P;Q)$ -corrected CC($P;Q$) energetics.

D. Trimethylenemethane

Our final example is trimethylenemethane, a fascinating non-Kekulé hydrocarbon examined as early as in 1948¹⁷³ and 1950,¹⁷⁴ in which four valence π electrons are delocalized over four closely spaced π -type orbitals. Assuming the D_{3h} symmetry, which is the symmetry of the minimum-energy structure on the ground-state triplet surface of trimethylenemethane, the four MOs of this system's valence π network consist of the nondegenerate $1a''_2$ orbital, the doubly degenerate $1e''$ shell, and the nondegenerate $2a''_2$ orbital. If one adopts the C_{2v} symmetry, relevant to the low-lying singlet states, which is also the largest Abelian subgroup of D_{3h} exploited in our CCSD, CR-CC(2,3), CCSDT, and CIQMC-driven CC(P) and CC($P;Q$) computations, the nondegenerate $1a''_2$ and $2a''_2$ orbitals in a D_{3h} description become the $1b_1$ and $3b_1$ MOs, respectively, whereas the degenerate $1e''$ shell splits into the $1a_2$ and $2b_1$ components.

The first experimental identification of trimethylenemethane dates back to 1966,¹⁷⁵ a definitive experimental verification, using electron paramagnetic resonance, of its triplet ground state was accomplished already in 1976,¹⁷⁶ and the electronic structure of trimethylenemethane has been well understood for decades (cf., e.g., Ref. 177 and references therein), but an accurate characterization of its triplet ground state and low-lying singlet states and energy separations between them continues to present a significant challenge to quantum chemistry approaches.^{52,115,116,123,135,136,178-201} The D_{3h} -symmetric triplet ground state, designated as $X^3A'_2$ (in a C_{2v} description adopted in this study, X^3B_2), which is dominated by the $|\{\text{core}\}(1a''_2)^2(1e''_1)^1(1e''_2)^1|$ configuration (in C_{2v} , $|\{\text{core}\}(1b_1)^2(1a_2)^1(2b_1)^1|$), is relatively easy to describe, but the next two states, which are the nearly degenerate singlets stabilized by the Jahn-Teller distortion that lifts their exact degeneracy in a D_{3h} description, are not. The lower of the two singlets, which is characterized by a C_s -symmetric minimum that can be approximated by a twisted C_{2v} structure and which is, therefore, usually designated as the A^1B_1 state, is an open-shell singlet that emerges from the $|\{\text{core}\}(1b_1)^2(1a_2)^1(2b_1)^1|$ configuration. The second singlet, labeled as the B^1A_1 state, is a C_{2v} -

symmetric multi-configurational state dominated by the $|\{\text{core}\}(1b_1)^2(1a_2)^2|$ and $|\{\text{core}\}(1b_1)^2(2b_1)^2|$ closed-shell determinants. The A^1B_1 state, although lower in energy compared to its B^1A_1 counterpart, has not been observed experimentally due to unfavorable Frank-Condon factors,^{193,202} so we do not consider it in this work. However, the second singlet, B^1A_1 , has been detected in photoelectron spectroscopy experiments reported in Refs. 202 and 203, which located it at 16.1 ± 0.1 kcal/mol above the $X^3A'_2$ ground state. Thus, following our previous deterministic, active-orbital-based, CC($P;Q$) work⁵² and the state-of-the-art DEA- and DIP-EOMCC computations with up to 4p2h and 4h2p excitations reported in Refs. 123, 135, and 136, in carrying out the CIQMC-driven CC(P) and CC($P;Q$) calculations discussed in this subsection and executing the accompanying CCSD, CR-CC(2,3), and CCSDT runs, we focused on the D_{3h} -symmetric triplet ground state, $X^3A'_2$, the C_{2v} -symmetric B^1A_1 singlet, and the adiabatic gap between them, adopting the geometries of the two states optimized using the spin-flip density functional theory (SF-DFT) and the 6-31G(d) basis in Ref. 115. In analogy to other organic biradicals discussed in this article, we employed the cc-pVDZ basis set, so that the parent CCSDT computations, needed to judge the performance of our semi-stochastic CC(P) and CC($P;Q$) methods, and the more expensive CC(P) and CC($P;Q$) calculations employing large, near-100%, fractions of triples in the relevant P spaces (captured in the later stages of the underlying CIQMC propagations) were not too difficult to execute on the computers available to us. As shown in our earlier deterministic CC($P;Q$) work,⁵² in which we tested the active-orbital-based CC(t;3) method, which recovers the CCSDT energetics to within small fractions of kilocalorie per mole, and as confirmed by the authors of Ref. 199, who managed to perform the CCSDT/cc-pVTZ calculations, the use of a larger cc-pVTZ basis changes the adiabatic $B^1A_1 - X^3A'_2$ gap by about 0.5–1 kcal/mol, i.e., the use of the cc-pVDZ basis is sufficient to draw meaningful conclusions regarding the performance of the semi-stochastic CC(P) and CC($P;Q$) approaches.

While the main goal of this study is to examine the efficiency of the CIQMC-driven CC($P;Q$) approaches in converging the CCSDT energetics, it is worth pointing out that the parent CCSDT calculations using the ROHF reference determinant for the $X^3A'_2$ state and the RHF reference for the more strongly correlated B^1A_1 state, in spite of their SR character, are capable of producing a reasonably accurate description of the adiabatic $B^1A_1 - X^3A'_2$ separation in trimethylenemethane. Indeed, the purely electronic $B^1A_1 - X^3A'_2$ gap, designated, in analogy to other singlet-triplet gaps considered in this work, as ΔE_{S-T} , resulting from the ROHF/RHF-based CCSDT/cc-pVDZ computations using the SF-DFT/6-31G(d) geometries of the $X^3A'_2$ and B^1A_1 states optimized in Ref. 115 is 21.7 kcal/mol⁵² (cf. Table VII). The corresponding experimentally derived result,

obtained by subtracting the zero-point vibrational energy correction $\Delta ZPVE$ resulting from the SF-DFT/6-31G(d) calculations reported in Ref. 115 from the experimental $B^1A_1 - X^3A_2'$ gap determined in Refs. 202 and 203, is 18.1 kcal/mol. The CCSDT/cc-pVDZ value of ΔE_{S-T} is not as accurate as the electronic $B^1A_1 - X^3A_2'$ gaps generated in the high-level DEA- and DIP-EOMCC calculations with the explicit inclusion of 4p2h and 4h2p correlations on top of CCSD, which produce 18–19 kcal/mol,^{123,135,136} but it is certainly much better than 46.1, 24.4, and 29.8 kcal/mol obtained with the ROHF/RHF-based CCSD, CCSD(T), and CR-CC(2,3) methods, respectively, when the cc-pVDZ basis set is employed⁵² [as demonstrated in Ref. 52, the use of a larger cc-pVTZ basis makes the CCSD, CCSD(T), and CR-CC(2,3) results even worse; the CCSD/cc-pVDZ and CR-CC(2,3)/cc-pVDZ values of ΔE_{S-T} are included in Table VII as the $\tau = 0$ $CC(P)$ and $CC(P;Q)$ data, respectively]. While much of the 3.6 kcal/mol difference between the electronic $B^1A_1 - X^3A_2'$ separation obtained in the ROHF/RHF-based CCSDT/cc-pVDZ calculations and its experimentally derived estimate of 18.1 kcal/mol determined in Ref. 115 is, most likely, a consequence of the neglect of T_4 clusters in the CCSDT approach, we should keep in mind that the latter estimate depends on the source of the information about the $\Delta ZPVE$ correction. For example, if one replaces the $\Delta ZPVE$ value obtained in the SF-DFT/6-31G(d) calculations reported in Ref. 115 by its CCSD(T)/6-311++G(2d,2p) estimate and accounts for the core polarization effects determined with the help of the CCSD(T)/cc-pCVQZ computations, combining the resulting information with the experimental $B^1A_1 - X^3A_2'$ separation determined in Refs. 202 and 203, the purely electronic, experimentally derived, adiabatic ΔE_{S-T} gap increases to 19.4 kcal/mol,¹⁹⁹ which differs from our CCSDT/cc-pVDZ result by 2.3 kcal/mol. On the other hand, as shown in Ref. 199, the CCSDT value of the adiabatic $B^1A_1 - X^3A_2'$ gap increases with the basis set too, to 23.1 kcal/mol when the cc-pVTZ basis is employed, which reinforces our view that without accounting for T_4 correlations one cannot bring the results of conventional SRCC computations to a close agreement with the experimentally derived data. While the examination of the role of T_4 clusters, basis set, geometries of the X^3A_2' and B^1A_1 states employed in the calculations, $\Delta ZPVE$ corrections, etc. would certainly be interesting, it would also be outside the scope of the present study. Thus, in the remainder of this subsection, we return to the analysis of the performance of the CIQMC-driven $CC(P;Q)$ approach and its $CC(P)$ counterpart, especially their ability to converge the parent CCSDT energetics when the cc-pVDZ basis is employed.

The results of our semi-stochastic $CC(P)$ /cc-pVDZ and $CC(P;Q)$ /cc-pVDZ computations for the X^3A_2' and B^1A_1 states of trimethylenemethane and the adiabatic gap between them, along with the associated CCSD, CR-CC(2,3), and CCSDT data, are summarized in Table VII

and Fig. 5. As in the case of cyclopentadienyl cation, to reduce the computational costs of the underlying CIQMC propagations, especially in their later stages, we resorted to the truncated *i*-CISDTQ-MC approach. In analogy to cyclobutadiene and cyclopentadienyl cation, we terminated our *i*-CISDTQ-MC propagations after 80000 $\delta\tau = 0.0001$ a.u. MC time steps, where the differences between the $CC(P;Q)$ and CCSDT energies of the X^3A_2' and B^1A_1 states fall below 1 microhartree. Consistent with the $CC(P)$, $CC(P;Q)$, and other SRCC calculations for trimethylenemethane reported in Table VII and Fig. 5, we used the ROHF determinant to initiate the *i*-CISDTQ-MC propagation for the D_{3h} -symmetric X^3A_2' (in C_{2v} , X^3B_2) state and the RHF determinant to initiate the *i*-CISDTQ-MC run for the C_{2v} -symmetric B^1A_1 state. The lists of triply excited determinants captured by the *i*-CISDTQ-MC runs at the various times $\tau > 0$, needed to construct the P spaces for the $CC(P)$ and $CC(P;Q)$ computations, were the $S_z = 1$ triples of the $B_2(C_{2v})$ symmetry in the case of the X^3A_2' state and the $S_z = 0$ triples of the $A_1(C_{2v})$ symmetry when considering the B^1A_1 state. The remaining triples not captured by *i*-CISDTQ-MC defined the corresponding Q spaces.

It is clear from the results presented in Table VII and Fig. 5 that the semi-stochastic $CC(P;Q)$ approach is very effective in converging the parent CCSDT energetics characterizing the X^3A_2' and B^1A_1 states of trimethylenemethane and the adiabatic gap between them. It offers substantial improvements in the results of the CR-CC(2,3) calculations in the early stages of the underlying *i*-CISDTQ-MC propagations, especially when the multi-configurational B^1A_1 state and the adiabatic $B^1A_1 - X^3A_2'$ separation ΔE_{S-T} , which are poorly described by CR-CC(2,3), are examined, while greatly accelerating the convergence of the $CC(P)$ energies toward CCSDT. Indeed, after 6000 $\delta\tau = 0.0001$ a.u. MC iterations, which is a very short propagation time engaging only $\sim 0.1\%$ of the total walker populations at $\tau = 8.0$ a.u., where we terminated our *i*-CISDTQ-MC runs (cf. Table S.5 of the supplementary material), and *i*-CISDTQ-MC capturing as little as 14–17% of all triply excited determinants, the semi-stochastic $CC(P;Q)$ methodology reduces the 13.370 millihartree difference between the CR-CC(2,3) and CCSDT energies of the B^1A_1 state and the 8.1 kcal/mol error in the CR-CC(2,3) value of the $B^1A_1 - X^3A_2'$ gap relative to CCSDT to 1.260 millihartree and 0.6 kcal/mol, respectively, which is a chemical accuracy regime. Interestingly, the *i*-CISDTQ-MC-based $CC(P;Q)$ value of ΔE_{S-T} obtained after 6000 MC iterations matches the quality of the $B^1A_1 - X^3A_2'$ gap resulting from the fully deterministic $CC(P;Q)$ calculations using the $CC(t;3)$ approach, which give a 0.5 kcal/mol error relative to CCSDT when the cc-pVDZ basis set is employed.⁵² After the additional 4000 MC time steps, where the *i*-CISDTQ-MC propagations for the X^3A_2' and B^1A_1 states are still very far from convergence and where the fractions of triples captured by

i-CISDTQ-MC increase to about 30%, the small errors relative to CCSDT characterizing the *i*-CISDTQ-MC-based $CC(P;Q)$ values of the energy of the B^1A_1 state and ΔE_{S-T} at $\tau = 0.6$ a.u. drop down by factors of 4–6, to 0.314 millihartree and 0.1 kcal/mol, respectively, illustrating how rapid the convergence of the CIQMC-driven $CC(P;Q)$ calculations toward the parent SRCC data can be. While the CR-CC(2,3) description of the $X^3A'_2$ state, which has a SR character, is much better than in the case of its strongly correlated B^1A_1 counterpart, the semi-stochastic $CC(P;Q)$ computations offer great improvements in this case too. They are, for example, capable of reducing the ~ 0.4 millihartree difference between the CR-CC(2,3) and CCSDT energies to a 0.1 millihartree level after 10000 MC iterations and *i*-CISDTQ-MC capturing less than 30% of all triples. In analogy to all other molecular examples considered in this article, the uncorrected $CC(P)$ values of the energies of the $X^3A'_2$ and B^1A_1 states and separation between them converge to their CCSDT limits too, but it is clear from Table VII and Fig. 5 that they do it at a much slower rate than their $CC(P;Q)$ counterparts. This can be illustrated by comparing the errors relative to CCSDT characterizing the $CC(P)$ and $CC(P;Q)$ energies of the $X^3A'_2$ and B^1A_1 states and separation between them obtained after 6000 MC iterations. They are more than 11 millihartree, about 21 millihartree, and almost 6 kcal/mol, respectively, in the former case and only 0.253 millihartree, 1.260 millihartree, and 0.6 kcal/mol, when the $CC(P)$ energies are corrected for the remaining T_3 correlations using the $CC(P;Q)$ approach. As explained in Section II, the $CC(P)$ energies converge to CCSDT more slowly than their $\delta(P;Q)$ -corrected $CC(P;Q)$ counterparts, since the initial, $\tau = 0$, $CC(P)$ calculation for a given electronic state is equivalent to CCSD, where $T_3 = 0$. The CIQMC-driven $CC(P;Q)$ calculations start from CR-CC(2,3), which provides information about T_3 clusters via noniterative corrections to CCSD. This once again emphasizes the benefits of using corrections $\delta(P;Q)$ in the context of the semi-stochastic $CC(P;Q)$ work.

IV. CONCLUSIONS

One of the most promising ideas in the area of converging high-level SRCC energetics without having to resort to the very expensive methods such as CCSDT or CCSDTQ has been the $CC(P;Q)$ formalism, originally introduced in Refs. 50–52, in which one solves the CC amplitude equations in a suitably defined subspace of the many-electron Hilbert space, called the P space, and then improves the resulting $CC(P)$ energies using the *a posteriori* corrections $\delta(P;Q)$ determined with the help of another subspace of the Hilbert space, referred to as the Q space. In addition to conventional choices of the P and Q spaces, which result in methods such as CR-CC(2,3),^{54–58} one can consider various unconventional ways of setting up these spaces in the $CC(P;Q)$

calculations.^{50–53,59,65,95–97,102} In this work, we have focused on the semi-stochastic formulation of the $CC(P;Q)$ formalism, introduced in Ref. 95 and further developed in Refs. 96 and 97, in which the leading higher-than-doubly excited determinants incorporated in the P space, needed to solve the $CC(P)$ equations, are identified, in an automated fashion, by the stochastic wave function propagations employing the CIQMC methodology of Refs. 86–90.

The specific objective of this study has been the investigation of the effectiveness of the semi-stochastic $CC(P;Q)$ approaches driven by *i*-FCIQMC and *i*-CISDTQ-MC propagations, which were used to capture the leading triply excited determinants for the inclusion in the respective P spaces, in converging the singlet–triplet gaps and the underlying total electronic energies resulting from the high-level CCSDT computations. Molecular systems that have been used to examine the ability of the semi-stochastic $CC(P;Q)$ methodology to recover the CCSDT energetics of the low-lying singlet and triplet states included the methylene, cyclobutadiene, cyclopentadienyl cation, and trimethylenemethane biradicals and a prototype magnetic system represented by the $(\text{HFH})^-$ ion. Cyclopentadienyl cation and trimethylenemethane are the largest polyatomic species that have been used in the semi-stochastic $CC(P;Q)$ calculations reported to date.

An accurate determination of the singlet–triplet gaps in the above five systems requires a well-balanced treatment of substantial nondynamical correlation effects, needed for a reliable description of the low-spin singlet states that have a manifestly MR character, and dynamical correlations of the high-spin triplet states, which are SR in nature. Within the conventional, particle-conserving, black-box SRCC framework, the only methods that can do this in a robust manner are the high-level CC approaches with a full treatment of T_n correlations with $n > 2$, beginning with CCSDT. The basic CCSD approximation, which ignores the T_n cluster components with $n > 2$ altogether, and the noniterative T_3 corrections to CCSD, including even CR-CC(2,3), which can handle selected MR situations, such as single bond breaking, fail. Putting aside the quasi-perturbative character of the majority of the existing triples corrections to CCSD, a significant part of the problem is their inability to capture the coupling between the low-rank T_1 and T_2 clusters with their higher-rank T_3 counterpart, which cannot be ignored when the low-lying singlet states of biradicals are considered. We have shown in this study that by relaxing T_1 and T_2 amplitudes in the presence of the T_3 component defined using the list of the leading triply excited determinants identified by the CIQMC propagations and using the $\delta(P;Q)$ corrections to account for the remaining T_3 correlations that are not described by the underlying $CC(P)$ calculations, the semi-stochastic $CC(P;Q)$ methodology provides an efficient mechanism for incorporating the coupling among the T_1 , T_2 , and T_3 clusters relevant to a reliable description of the singlet–triplet gaps in biradicals, while capturing the vast ma-

majority of the many-electron correlation effects included in the parent CCSDT computations. In particular, we have demonstrated that the semi-stochastic $CC(P;Q)$ calculations are capable of reaching millihartree or submillihartree accuracy levels relative to the parent CCSDT results, including total electronic energies of the lowest singlet and triplet states and adiabatic as well as vertical gaps between them, with small (typically about 20–30%; sometimes even less) fractions of triply excited determinants captured in the early stages of the underlying CIQMC propagations and with tiny walker populations that are orders of magnitude smaller than the total numbers of walkers required to converge them. We have also demonstrated the vital role of the noniterative corrections $\delta(P;Q)$ in accelerating and, in the case of the singlet–triplet gap values, smoothing convergence of the corresponding $CC(P)$ energetics toward CCSDT.

The numerical results and analyses reported in this article encourage us to pursue the semi-stochastic $CC(P;Q)$ methodology even further. Putting aside the need for improving the computational efficiency of our CIQMC-driven $CC(P;Q)$ codes, so that we could consider larger molecular problems than those considered in this study, it would be interesting to examine if our semi-stochastic $CC(P;Q)$ computations, including those discussed in this work, could take advantage of the recent advances in CIQMC, such as the adaptive CIQMC algorithm of Refs. 89 and 90 that might replace the *i*-CIQMC approaches that we have used so far. As implied by the remarks made in Section III, some of the biradicals considered in this work might benefit from an accurate description of T_3 as well as T_4 correlations. It would, therefore, be interesting to examine if one could improve the results presented in this work by using the semi-stochastic $CC(P;Q)$ approaches that aim at converging the CCSDTQ energetics, such as those discussed in Ref. 97. Last, but not least, we have started developing extensions of the semi-stochastic $CC(P)$ and $CC(P;Q)$ approaches, pursued in Refs. 95 and 97 and this study, and their EOMCC analogs^{96,98} to the particle-nonconserving EOMCC models, especially EA/IP-EOMCC and DEA/DIP-EOMCC. As pointed out in this article, and as shown in Refs. 123–125, 135, and 136, the deterministic DEA/DIP-EOMCC approaches with the explicit inclusion of 4p2h and 4h2p components of the corresponding electron attaching and ionizing operators on top of CCSD can provide a nearly exact description of the singlet–triplet in biradical species, so it will be interesting if their semi-stochastic counterparts can do the same.

SUPPLEMENTARY MATERIAL

See the supplementary material for the information about the total numbers of walkers characterizing the *i*-FCIQMC [methylene, $(\text{HFH})^-$, cyclobutadiene] and *i*-CISDTQ-MC (cyclopentadienyl cation, trimethylenemethane) propagations carried out in this study.

ACKNOWLEDGMENTS

This work has been supported by the Chemical Sciences, Geosciences and Biosciences Division, Office of Basic Energy Sciences, Office of Science, U.S. Department of Energy (Grant No. DE-FG02-01ER15228 to P.P.) and the National Science Foundation (Grant No. CHE-1763371 to P.P.). The computational resources provided by the Institute for Cyber-Enabled Research at Michigan State University are gratefully acknowledged too.

DATA AVAILABILITY

The data that support the findings of this study are available within the article and its supplementary material.

- ¹B. O. Roos, *Adv. Chem. Phys.* **69**, 399 (1987).
- ²M. W. Schmidt and M. S. Gordon, *Annu. Rev. Phys. Chem.* **49**, 233 (1998).
- ³P. G. Szalay, T. Müller, G. Gidofalvi, H. Lischka, and R. Shepard, *Chem. Rev.* **112**, 108 (2012).
- ⁴D. Roca-Sanjuán, F. Aquilante, and R. Lindh, *WIREs Comput. Mol. Sci.* **2**, 585 (2012).
- ⁵S. Chattopadhyay, R. K. Chaudhuri, U. S. Mahapatra, A. Ghosh, and S. S. Ray, *WIREs Comput. Mol. Sci.* **6**, 266 (2016).
- ⁶D. I. Lyakh, M. Musiał, V. F. Lotrich, and R. J. Bartlett, *Chem. Rev.* **112**, 182 (2012).
- ⁷P. Piecuch and K. Kowalski, *Int. J. Mol. Sci.* **3**, 676 (2002).
- ⁸F. A. Evangelista, *J. Chem. Phys.* **149**, 030901 (2018).
- ⁹F. Coester, *Nucl. Phys.* **7**, 421 (1958).
- ¹⁰F. Coester and H. Kümmel, *Nucl. Phys.* **17**, 477 (1960).
- ¹¹J. Čížek, *J. Chem. Phys.* **45**, 4256 (1966).
- ¹²J. Čížek, *Adv. Chem. Phys.* **14**, 35 (1969).
- ¹³J. Paldus, J. Čížek, and I. Shavitt, *Phys. Rev. A* **5**, 50 (1972).
- ¹⁴J. Paldus and X. Li, *Adv. Chem. Phys.* **110**, 1 (1999).
- ¹⁵R. J. Bartlett and M. Musiał, *Rev. Mod. Phys.* **79**, 291 (2007).
- ¹⁶G. D. Purvis, III and R. J. Bartlett, *J. Chem. Phys.* **76**, 1910 (1982).
- ¹⁷J. M. Cullen and M. C. Zerner, *J. Chem. Phys.* **77**, 4088 (1982).
- ¹⁸G. E. Scuseria, A. C. Scheiner, T. J. Lee, J. E. Rice, and H. F. Schaefer, III, *J. Chem. Phys.* **86**, 2881 (1987).
- ¹⁹P. Piecuch and J. Paldus, *Int. J. Quantum Chem.* **36**, 429 (1989).
- ²⁰M. R. Hoffmann and H. F. Schaefer, III, *Adv. Quantum Chem.* **18**, 207 (1986).
- ²¹J. Noga and R. J. Bartlett, *J. Chem. Phys.* **86**, 7041 (1987), **89**, 3401 (1988) [Erratum].
- ²²G. E. Scuseria and H. F. Schaefer, III, *Chem. Phys. Lett.* **152**, 382 (1988).
- ²³J. D. Watts and R. J. Bartlett, *J. Chem. Phys.* **93**, 6104 (1990).
- ²⁴N. Oliphant and L. Adamowicz, *J. Chem. Phys.* **95**, 6645 (1991).
- ²⁵S. A. Kucharski and R. J. Bartlett, *Theor. Chim. Acta* **80**, 387 (1991).
- ²⁶S. A. Kucharski and R. J. Bartlett, *J. Chem. Phys.* **97**, 4282 (1992).
- ²⁷P. Piecuch and L. Adamowicz, *J. Chem. Phys.* **100**, 5792 (1994).
- ²⁸K. Emrich, *Nucl. Phys. A* **351**, 379 (1981).
- ²⁹J. Geertsen, M. Rittby, and R. J. Bartlett, *Chem. Phys. Lett.* **164**, 57 (1989).
- ³⁰J. F. Stanton and R. J. Bartlett, *J. Chem. Phys.* **98**, 7029 (1993).
- ³¹K. Kowalski and P. Piecuch, *J. Chem. Phys.* **115**, 643 (2001).
- ³²K. Kowalski and P. Piecuch, *Chem. Phys. Lett.* **347**, 237 (2001).
- ³³S. A. Kucharski, M. Włoch, M. Musiał, and R. J. Bartlett, *J. Chem. Phys.* **115**, 8263 (2001).

- ³⁴M. Kállay and J. Gauss, *J. Chem. Phys.* **121**, 9257 (2004).
- ³⁵S. Hirata, *J. Chem. Phys.* **121**, 51 (2004).
- ³⁶H. J. Monkhorst, *Int. J. Quantum Chem. Symp.* **11**, 421 (1977).
- ³⁷E. Dalgaard and H. J. Monkhorst, *Phys. Rev. A* **28**, 1217 (1983).
- ³⁸D. Mukherjee and P. K. Mukherjee, *Chem. Phys.* **39**, 325 (1979).
- ³⁹H. Sekino and R. J. Bartlett, *Int. J. Quantum Chem. Symp.* **18**, 255 (1984).
- ⁴⁰M. Takahashi and J. Paldus, *J. Chem. Phys.* **85**, 1486 (1986).
- ⁴¹H. Koch and P. Jørgensen, *J. Chem. Phys.* **93**, 3333 (1990).
- ⁴²H. Koch, H. J. A. Jensen, P. Jørgensen, and T. Helgaker, *J. Chem. Phys.* **93**, 3345 (1990).
- ⁴³A. E. Kondo, P. Piecuch, and J. Paldus, *J. Chem. Phys.* **102**, 6511 (1995).
- ⁴⁴A. E. Kondo, P. Piecuch, and J. Paldus, *J. Chem. Phys.* **104**, 8566 (1996).
- ⁴⁵K. Raghavachari, G. W. Trucks, J. A. Pople, and M. Head-Gordon, *Chem. Phys. Lett.* **157**, 479 (1989).
- ⁴⁶J. D. Watts, J. Gauss, and R. J. Bartlett, *J. Chem. Phys.* **98**, 8718 (1993).
- ⁴⁷P. Piecuch, K. Kowalski, I. S. O. Pimienta, and M. J. McGuire, *Int. Rev. Phys. Chem.* **21**, 527 (2002).
- ⁴⁸P. Piecuch, K. Kowalski, I. S. O. Pimienta, P.-D. Fan, M. Lodriguito, M. J. McGuire, S. A. Kucharski, T. Kuś, and M. Musiał, *Theor. Chem. Acc.* **112**, 349 (2004).
- ⁴⁹P. Piecuch, *Mol. Phys.* **108**, 2987 (2010).
- ⁵⁰J. Shen and P. Piecuch, *Chem. Phys.* **401**, 180 (2012).
- ⁵¹J. Shen and P. Piecuch, *J. Chem. Phys.* **136**, 144104 (2012).
- ⁵²J. Shen and P. Piecuch, *J. Chem. Theory Comput.* **8**, 4968 (2012).
- ⁵³N. P. Bauman, J. Shen, and P. Piecuch, *Mol. Phys.* **115**, 2860 (2017).
- ⁵⁴P. Piecuch and M. Włoch, *J. Chem. Phys.* **123**, 224105 (2005).
- ⁵⁵P. Piecuch, M. Włoch, J. R. Gour, and A. Kinal, *Chem. Phys. Lett.* **418**, 467 (2006).
- ⁵⁶M. Włoch, M. D. Lodriguito, P. Piecuch, and J. R. Gour, *Mol. Phys.* **104**, 2149 (2006), **104**, 2991 (2006) [Erratum].
- ⁵⁷M. Włoch, J. R. Gour, and P. Piecuch, *J. Phys. Chem. A* **111**, 11359 (2007).
- ⁵⁸P. Piecuch, J. R. Gour, and M. Włoch, *Int. J. Quantum Chem.* **108**, 2128 (2008).
- ⁵⁹I. Magoulas, N. P. Bauman, J. Shen, and P. Piecuch, *J. Phys. Chem. A* **122**, 1350 (2018).
- ⁶⁰P. Piecuch, M. Włoch, and A. J. C. Varandas, in *Topics in the Theory of Chemical and Physical Systems*, Progress in Theoretical Chemistry and Physics, Vol. 16, edited by S. Lahmar, J. Maruani, S. Wilson, and G. Delgado-Barrio (Springer, Dordrecht, 2007) pp. 63–121.
- ⁶¹P. Piecuch, M. Włoch, and A. J. C. Varandas, *Theor. Chem. Acc.* **120**, 59 (2008).
- ⁶²M. Horoi, J. R. Gour, M. Włoch, M. D. Lodriguito, B. A. Brown, and P. Piecuch, *Phys. Rev. Lett.* **98**, 112501 (2007).
- ⁶³Y. Ge, M. S. Gordon, and P. Piecuch, *J. Chem. Phys.* **127**, 174106 (2007).
- ⁶⁴Y. Ge, M. S. Gordon, P. Piecuch, M. Włoch, and J. R. Gour, *J. Phys. Chem. A* **112**, 11873 (2008).
- ⁶⁵S. H. Yuwono, I. Magoulas, J. Shen, and P. Piecuch, *Mol. Phys.* **117**, 1486 (2019).
- ⁶⁶P. Piecuch and K. Kowalski, in *Computational Chemistry: Reviews of Current Trends*, Vol. 5, edited by J. Leszczyński (World Scientific, Singapore, 2000) pp. 1–104.
- ⁶⁷K. Kowalski and P. Piecuch, *J. Chem. Phys.* **113**, 18 (2000).
- ⁶⁸K. Kowalski and P. Piecuch, *J. Chem. Phys.* **122**, 074107 (2005).
- ⁶⁹S. Hirata, M. Nooijen, I. Grabowski, and R. J. Bartlett, *J. Chem. Phys.* **114**, 3919 (2001), **115**, 3967 (2001) [Erratum].
- ⁷⁰S. Hirata, P.-D. Fan, A. A. Auer, M. Nooijen, and P. Piecuch, *J. Chem. Phys.* **121**, 12197 (2004).
- ⁷¹S. R. Gwaltney and M. Head-Gordon, *Chem. Phys. Lett.* **323**, 21 (2000).
- ⁷²S. R. Gwaltney and M. Head-Gordon, *J. Chem. Phys.* **115**, 2014 (2001).
- ⁷³J. F. Stanton, *Chem. Phys. Lett.* **281**, 130 (1997).
- ⁷⁴T. D. Crawford and J. F. Stanton, *Int. J. Quantum Chem.* **70**, 601 (1998).
- ⁷⁵S. A. Kucharski and R. J. Bartlett, *J. Chem. Phys.* **108**, 5243 (1998).
- ⁷⁶A. G. Taube and R. J. Bartlett, *J. Chem. Phys.* **128**, 044110 (2008).
- ⁷⁷A. G. Taube and R. J. Bartlett, *J. Chem. Phys.* **128**, 044111 (2008).
- ⁷⁸J. J. Eriksen, K. Kristensen, T. Kjærgaard, P. Jørgensen, and J. Gauss, *J. Chem. Phys.* **140**, 064108 (2014).
- ⁷⁹J. J. Eriksen, P. Jørgensen, J. Olsen, and J. Gauss, *J. Chem. Phys.* **140**, 174114 (2014).
- ⁸⁰N. Oliphant and L. Adamowicz, *J. Chem. Phys.* **94**, 1229 (1991).
- ⁸¹N. Oliphant and L. Adamowicz, *J. Chem. Phys.* **96**, 3739 (1992).
- ⁸²P. Piecuch, N. Oliphant, and L. Adamowicz, *J. Chem. Phys.* **99**, 1875 (1993).
- ⁸³P. Piecuch and L. Adamowicz, *J. Chem. Phys.* **102**, 898 (1995).
- ⁸⁴L. Adamowicz, P. Piecuch, and K. B. Ghose, *Mol. Phys.* **94**, 225 (1998).
- ⁸⁵P. Piecuch, S. A. Kucharski, and R. J. Bartlett, *J. Chem. Phys.* **110**, 6103 (1999).
- ⁸⁶G. H. Booth, A. J. W. Thom, and A. Alavi, *J. Chem. Phys.* **131**, 054106 (2009).
- ⁸⁷D. Cleland, G. H. Booth, and A. Alavi, *J. Chem. Phys.* **132**, 041103 (2010).
- ⁸⁸W. Dobrautz, S. D. Smart, and A. Alavi, *J. Chem. Phys.* **151**, 094104 (2019).
- ⁸⁹K. Ghanem, A. Y. Lozovoi, and A. Alavi, *J. Chem. Phys.* **151**, 224108 (2019).
- ⁹⁰K. Ghanem, K. Guther, and A. Alavi, *J. Chem. Phys.* **153**, 224115 (2020).
- ⁹¹A. J. W. Thom, *Phys. Rev. Lett.* **105**, 263004 (2010).
- ⁹²R. S. T. Franklin, J. S. Spencer, A. Zoccante, and A. J. W. Thom, *J. Chem. Phys.* **144**, 044111 (2016).
- ⁹³J. S. Spencer and A. J. W. Thom, *J. Chem. Phys.* **144**, 084108 (2016).
- ⁹⁴C. J. C. Scott and A. J. W. Thom, *J. Chem. Phys.* **147**, 124105 (2017).
- ⁹⁵J. E. Deustua, J. Shen, and P. Piecuch, *Phys. Rev. Lett.* **119**, 223003 (2017).
- ⁹⁶S. H. Yuwono, A. Chakraborty, J. E. Deustua, J. Shen, and P. Piecuch, *Mol. Phys.* **118**, e1817592 (2020).
- ⁹⁷J. E. Deustua, J. Shen, and P. Piecuch, *J. Chem. Phys.* **154**, 124103 (2021).
- ⁹⁸J. E. Deustua, S. H. Yuwono, J. Shen, and P. Piecuch, *J. Chem. Phys.* **150**, 111101 (2019).
- ⁹⁹B. Huron, J. P. Malrieu, and P. Rancurel, *J. Chem. Phys.* **58**, 5745 (1973).
- ¹⁰⁰Y. Garniron, A. Scemama, P.-F. Loos, and M. Caffarel, *J. Chem. Phys.* **147**, 034101 (2017).
- ¹⁰¹Y. Garniron, T. Applencourt, K. Gasperich, A. Benali, A. Ferté, J. Paquier, B. Pradines, R. Assaraf, P. Reinhardt, J. Toulouse, P. Barbaresco, N. Renon, G. David, J.-P. Malrieu, M. Vénil, M. Caffarel, P.-F. Loos, E. Giner, and A. Scemama, *J. Chem. Theory Comput.* **15**, 3591 (2019).
- ¹⁰²K. Gururangan, J. E. Deustua, J. Shen, and P. Piecuch, *J. Chem. Phys.* **155**, 174114 (2021).
- ¹⁰³S. Pedersen, J. L. Herek, and A. H. Zewail, *Science* **266**, 1359 (1994).
- ¹⁰⁴D. Cho, K. C. Ko, and J. Y. Lee, *Int. J. Quantum Chem.* **116**, 578 (2016).
- ¹⁰⁵T. Sugawara, H. Komatsu, and K. Suzuki, *Chem. Soc. Rev.* **40**, 3105 (2011).
- ¹⁰⁶S. Sanvito, *Chem. Soc. Rev.* **40**, 3336 (2011).
- ¹⁰⁷M. Nakano and B. Champagne, *WIREs Comput. Mol. Sci.* **6**, 198 (2016).
- ¹⁰⁸M. Z. Zgierski, S. Patchkovskii, and E. C. Lim, *J. Chem. Phys.* **123**, 081101 (2005).

- ¹⁰⁹M. Z. Zgierski, S. Patchkovskii, T. Fujiwara, and E. C. Lim, *J. Phys. Chem. A* **109**, 9384 (2005).
- ¹¹⁰W. Park, J. Shen, S. Lee, P. Piecuch, M. Filatov, and C. H. Choi, *J. Phys. Chem. Lett.* **12**, 9720 (2021).
- ¹¹¹T. Minami and M. Nakano, *J. Phys. Chem. Lett.* **3**, 145 (2012).
- ¹¹²G. J. Hedley, A. Ruseckas, and I. D. W. Samuel, *Chem. Rev.* **117**, 796 (2017).
- ¹¹³J. Niklas and O. G. Poluektov, *Adv. Energy Mat.* **7**, 1602226 (2017).
- ¹¹⁴J. R. Hart, A. K. Rappe, S. M. Gorun, and T. H. Upton, *J. Phys. Chem.* **96**, 6264 (1992).
- ¹¹⁵L. V. Slipchenko and A. I. Krylov, *J. Chem. Phys.* **117**, 4694 (2002).
- ¹¹⁶X. Li and J. Paldus, *J. Chem. Phys.* **129**, 174101 (2008).
- ¹¹⁷O. Demel, K. R. Shamasundar, L. Kong, and M. Nooijen, *J. Phys. Chem. A* **112**, 11895 (2008).
- ¹¹⁸T. Saito, S. Nishihara, S. Yamanaka, Y. Kitagawa, T. Kawakami, S. Yamada, H. Isobe, M. Okumura, and K. Yamaguchi, *Theor. Chem. Acc.* **130**, 749 (2011).
- ¹¹⁹D. H. Ess, E. R. Johnson, X. Hu, and W. Yang, *J. Phys. Chem. A* **115**, 76 (2011).
- ¹²⁰M. Abe, *Chem. Rev.* **113**, 7011 (2013).
- ¹²¹A. J. Garza, C. A. Jiménez-Hoyos, and G. E. Scuseria, *J. Chem. Phys.* **140**, 244102 (2014).
- ¹²²C. U. Ibeji and D. Ghosh, *Phys. Chem. Chem. Phys.* **17**, 9849 (2015).
- ¹²³A. O. Ajala, J. Shen, and P. Piecuch, *J. Phys. Chem. A* **121**, 3469 (2017).
- ¹²⁴S. J. Stoneburner, J. Shen, A. O. Ajala, P. Piecuch, D. G. Truhlar, and L. Gagliardi, *J. Chem. Phys.* **147**, 164120 (2017).
- ¹²⁵J. Shen and P. Piecuch, *Mol. Phys.* **119**, e1966534 (2021).
- ¹²⁶S. Gulania, E. F. Kjørstad, J. F. Stanton, H. Koch, and A. I. Krylov, *J. Chem. Phys.* **154**, 114115 (2021).
- ¹²⁷M. Nooijen and R. J. Bartlett, *J. Chem. Phys.* **106**, 6441 (1997).
- ¹²⁸M. Władysławski and M. Nooijen, in *Low-Lying Potential Energy Surfaces*, ACS Symposium Series, Vol. 828, edited by M. R. Hoffmann and K. G. Dyall (American Chemical Society, Washington, D.C., 2002) pp. 65–92.
- ¹²⁹M. Nooijen, *Int. J. Mol. Sci.* **3**, 656 (2002).
- ¹³⁰K. W. Sattelmeyer, H. F. Schaefer, III, and J. F. Stanton, *Chem. Phys. Lett.* **378**, 42 (2003).
- ¹³¹M. Musiał, A. Perera, and R. J. Bartlett, *J. Chem. Phys.* **134**, 114108 (2011).
- ¹³²M. Musiał, S. A. Kucharski, and R. J. Bartlett, *J. Chem. Theory Comput.* **7**, 3088 (2011).
- ¹³³T. Kuś and A. I. Krylov, *J. Chem. Phys.* **135**, 084109 (2011).
- ¹³⁴T. Kuś and A. I. Krylov, *J. Chem. Phys.* **136**, 244109 (2012).
- ¹³⁵J. Shen and P. Piecuch, *J. Chem. Phys.* **138**, 194102 (2013).
- ¹³⁶J. Shen and P. Piecuch, *Mol. Phys.* **112**, 868 (2014).
- ¹³⁷P. Piecuch, J. R. Gour, and M. Włoch, *Int. J. Quantum Chem.* **109**, 3268 (2009).
- ¹³⁸G. Fradelos, J. J. Lutz, T. A. Wesolowski, P. Piecuch, and M. Włoch, *J. Chem. Theory Comput.* **7**, 1647 (2011).
- ¹³⁹K. Jankowski, J. Paldus, and P. Piecuch, *Theor. Chim. Acta* **80**, 223 (1991).
- ¹⁴⁰T. H. Dunning, Jr., *J. Chem. Phys.* **90**, 1007 (1989).
- ¹⁴¹R. A. Kendall, T. H. Dunning, Jr., and R. J. Harrison, *J. Chem. Phys.* **96**, 6796 (1992).
- ¹⁴²W. J. Hehre, R. Ditchfield, and J. A. Pople, *J. Chem. Phys.* **56**, 2257 (1972).
- ¹⁴³P. C. Hariharan and J. A. Pople, *Theor. Chim. Acta* **28**, 213 (1973).
- ¹⁴⁴M. W. Schmidt, K. K. Baldrige, J. A. Boatz, S. T. Elbert, M. S. Gordon, J. H. Jensen, S. Koseki, N. Matsunaga, K. A. Nguyen, S. Su, T. L. Windus, M. Dupuis, and J. A. Montgomery, Jr., *J. Comput. Chem.* **14**, 1347 (1993).
- ¹⁴⁵G. M. J. Barca, C. Bertoni, L. Carrington, D. Datta, N. De Silva, J. E. Deustua, D. G. Fedorov, J. R. Gour, A. O. Gunina, E. Guidez, T. Harville, S. Irlé, J. Ivanic, K. Kowalski, S. S. Leang, H. Li, W. Li, J. J. Lutz, I. Magoulas, J. Mato, V. Mironov, H. Nakata, B. Q. Pham, P. Piecuch, D. Poole, S. R. Pruitt, A. P. Rendell, L. B. Roskop, K. Ruedenberg, T. Sattasathuchana, M. W. Schmidt, J. Shen, L. Slipchenko, M. Sosonkina, V. Sundriyal, A. Tiwari, J. L. G. Vallejo, B. Westheimer, M. Włoch, P. Xu, F. Zahariev, and M. S. Gordon, *J. Chem. Phys.* **152**, 154102 (2020).
- ¹⁴⁶J. S. Spencer, N. S. Blunt, W. A. Vigor, F. D. Malone, W. M. C. Foulkes, J. J. Shepherd, and A. J. W. Thom, *J. Open Res. Softw.* **3**, e9 (2015).
- ¹⁴⁷J. S. Spencer, N. S. Blunt, S. Choi, J. Etrych, M.-A. Filip, W. M. C. Foulkes, R. S. T. Franklin, W. J. Handley, F. D. Malone, V. A. Neufeld, R. Di Remigio, T. W. Rogers, C. J. C. Scott, J. J. Shepherd, W. A. Vigor, J. Weston, R. Xu, and A. J. W. Thom, *J. Chem. Theory Comput.* **15**, 1728 (2019).
- ¹⁴⁸T. H. Dunning, Jr., *J. Chem. Phys.* **55**, 716 (1971).
- ¹⁴⁹C. D. Sherrill, M. L. Leininger, T. J. Van Huis, and H. F. Schaefer, III, *J. Chem. Phys.* **108**, 1040 (1998).
- ¹⁵⁰C. W. Bauschlicher, Jr. and P. R. Taylor, *J. Chem. Phys.* **85**, 6510 (1986).
- ¹⁵¹C. W. Bauschlicher, Jr., S. R. Langhoff, and P. R. Taylor, *J. Chem. Phys.* **87**, 387 (1987).
- ¹⁵²A. D. McLean, P. R. Bunker, R. M. Escibano, and P. Jensen, *J. Chem. Phys.* **87**, 2166 (1987).
- ¹⁵³D. C. Comeau, I. Shavitt, P. Jensen, and P. R. Bunker, *J. Chem. Phys.* **90**, 6491 (1989).
- ¹⁵⁴D. B. Knowles, J. R. Alvarez-Collado, G. Hirsch, and R. J. Buenker, *J. Chem. Phys.* **92**, 585 (1990).
- ¹⁵⁵X. Li, P. Piecuch, and J. Paldus, *Chem. Phys. Lett.* **224**, 267 (1994).
- ¹⁵⁶P. Piecuch, X. Li, and J. Paldus, *Chem. Phys. Lett.* **230**, 377 (1994).
- ¹⁵⁷A. Balková and R. J. Bartlett, *J. Chem. Phys.* **102**, 7116 (1995).
- ¹⁵⁸X. Li and J. Paldus, *J. Chem. Phys.* **124**, 174101 (2006).
- ¹⁵⁹J. R. Gour, P. Piecuch, and M. Włoch, *Mol. Phys.* **108**, 2633 (2010).
- ¹⁶⁰P. Jensen and P. R. Bunker, *J. Chem. Phys.* **89**, 1327 (1988).
- ¹⁶¹E. R. Davidson, D. Feller, and P. Phillips, *Chem. Phys. Lett.* **76**, 416 (1980).
- ¹⁶²N. C. Handy, Y. Yamaguchi, and H. F. Schaefer, III, *J. Chem. Phys.* **84**, 4481 (1986).
- ¹⁶³J. Shen, Z. Kou, E. Xu, and S. Li, *J. Chem. Phys.* **134**, 044134 (2011).
- ¹⁶⁴H. Schurkus, D.-T. Chen, H.-P. Cheng, G. Chan, and J. Stanton, *J. Chem. Phys.* **152**, 234115 (2020).
- ¹⁶⁵P. G. Szalay and R. J. Bartlett, *Chem. Phys. Lett.* **214**, 481 (1993).
- ¹⁶⁶P. G. Szalay and R. J. Bartlett, *J. Chem. Phys.* **103**, 3600 (1995).
- ¹⁶⁷M. Eckert-Maksić, M. Vazdar, M. Barbatti, H. Lischka, and Z. B. Maksić, *J. Chem. Phys.* **125**, 064310 (2006).
- ¹⁶⁸A. Balková and R. J. Bartlett, *J. Chem. Phys.* **101**, 8972 (1994).
- ¹⁶⁹S. V. Levchenko and A. I. Krylov, *J. Chem. Phys.* **120**, 175 (2004).
- ¹⁷⁰P. M. Zimmerman, *J. Phys. Chem. A* **121**, 4712 (2017).
- ¹⁷¹J.-N. Boyn and D. A. Mazziotti, *J. Chem. Phys.* **154**, 134103 (2021).
- ¹⁷²E. Monino, M. Boggio-Pasqua, A. Scemama, D. Jacquemin, and P.-F. Loos, *ArXiv:2204.05098* (2022).
- ¹⁷³C. A. Coulson, *J. Chim. Phys. Phys.-Chim. Biol.* **45**, 243 (1948).
- ¹⁷⁴H. C. Longuet-Higgins, *J. Chem. Phys.* **18**, 265 (1950).
- ¹⁷⁵P. Dowd, *J. Am. Chem. Soc.* **88**, 2587 (1966).
- ¹⁷⁶R. J. Baseman, D. W. Pratt, M. Chow, and P. Dowd, *J. Am. Chem. Soc.* **98**, 5726 (1976).
- ¹⁷⁷W. T. Borden and E. R. Davidson, *Acc. Chem. Res.* **14**, 69 (1981).
- ¹⁷⁸D. R. Yarkony and H. F. Schaefer, III, *J. Am. Chem. Soc.* **96**, 3754 (1974).
- ¹⁷⁹W. J. Hehre, L. Salem, and M. R. Willcott, *J. Am. Chem. Soc.* **96**, 4328 (1974).

- ¹⁸⁰J. H. Davis and W. A. Goddard, III, *J. Am. Chem. Soc.* **99**, 4242 (1977).
- ¹⁸¹D. M. Hood, R. M. Pitzer, and H. F. Schaefer, III, *J. Am. Chem. Soc.* **100**, 2227 (1978).
- ¹⁸²D. M. Hood, H. F. Schaefer, III, and R. M. Pitzer, *J. Am. Chem. Soc.* **100**, 8009 (1978).
- ¹⁸³D. A. Dixon, R. Foster, T. A. Halgren, and W. N. Lipscomb, *J. Am. Chem. Soc.* **100**, 1359 (1978).
- ¹⁸⁴D. Feller, W. T. Borden, and E. R. Davidson, *J. Chem. Phys.* **74**, 2256 (1981).
- ¹⁸⁵S. B. Auster, R. M. Pitzer, and M. S. Platz, *J. Am. Chem. Soc.* **104**, 3812 (1982).
- ¹⁸⁶W. T. Borden, E. R. Davidson, and D. Feller, *Tetrahedron* **38**, 737 (1982).
- ¹⁸⁷P. M. Lahti, A. R. Rossi, and J. A. Berson, *J. Am. Chem. Soc.* **107**, 2273 (1985).
- ¹⁸⁸A. Skanche, L. J. Schaad, and B. A. Hess, Jr., *J. Am. Chem. Soc.* **110**, 5315 (1988).
- ¹⁸⁹S. Olivella and J. Salvador, *Int. J. Quantum Chem.* **37**, 713 (1990).
- ¹⁹⁰T. P. Radhakrishnan, *Tetrahedron Lett.* **32**, 4601 (1991).
- ¹⁹¹A. S. Ichimura, N. Koga, and H. Iwamura, *J. Phys. Org. Chem.* **7**, 207 (1994).
- ¹⁹²W. T. Borden, *Mol. Cryst. Liq. Cryst.* **232**, 195 (1993).
- ¹⁹³C. J. Cramer and B. A. Smith, *J. Phys. Chem.* **100**, 9664 (1996).
- ¹⁹⁴B. Ma and H. F. Schaefer, III, *Chem. Phys.* **207**, 31 (1996).
- ¹⁹⁵L. V. Slipchenko and A. I. Krylov, *J. Chem. Phys.* **118**, 6874 (2003).
- ¹⁹⁶L. V. Slipchenko and A. I. Krylov, *J. Chem. Phys.* **123**, 084107 (2005).
- ¹⁹⁷J. Brabec and J. Pittner, *J. Phys. Chem. A* **110**, 11765 (2006).
- ¹⁹⁸J. Shen, T. Fang, S. Li, and Y. Jiang, *J. Phys. Chem. A* **112**, 12518 (2008).
- ¹⁹⁹A. Perera, R. W. Molt, Jr., V. F. Lotrich, and R. J. Bartlett, *Theor. Chem. Acc.* **133**, 1514 (2014).
- ²⁰⁰S. Sinha Ray, S. Manna, A. Ghosh, R. K. Chaudhuri, and S. Chattopadhyay, *Int. J. Quantum Chem.* **119**, e25776 (2019).
- ²⁰¹S. Chattopadhyay, *ACS Omega* **6**, 1668 (2021).
- ²⁰²P. G. Wenthold, J. Hu, R. R. Squires, and W. C. Lineberger, *J. Am. Chem. Soc.* **118**, 475 (1996).
- ²⁰³P. G. Wenthold, J. Hu, R. R. Squires, and W. C. Lineberger, *J. Am. Soc. Mass Spectrom.* **10**, 800 (1999).

TABLE I. Convergence of the $CC(P)$ and $CC(P;Q)$ energies of the X^3B_1 and A^1A_1 states of methylene, as described by the aug-cc-pVTZ basis set, and of the corresponding adiabatic singlet–triplet gaps toward their parent CCSDT values. The geometries of the X^3B_1 and A^1A_1 states, optimized in the FCI calculations using the TZ2P basis set, were taken from Ref. 149. The P spaces used in the $CC(P)$ and $CC(P;Q)$ calculations were defined as all singly and doubly excited determinants and subsets of triply excited determinants extracted from the i -FCIQMC propagations with $\delta\tau = 0.0001$ a.u. The Q spaces used to determine the $CC(P;Q)$ corrections consisted of the triply excited determinants not captured by the corresponding i -FCIQMC runs. The i -FCIQMC calculations preceding the $CC(P)$ and $CC(P;Q)$ steps were initiated by placing 1500 walkers on the ROHF (X^3B_1 state) and RHF (A^1A_1 state) reference determinants and the n_a parameter of the initiator algorithm was set at 3. In all post-Hartree–Fock calculations, the lowest core orbital was kept frozen and the spherical components of d and f orbitals were employed throughout.

MC Iterations	X^3B_1			A^1A_1			$A^1A_1 - X^3B_1$	
	P^a	$(P;Q)^a$	%T ^b	P^a	$(P;Q)^a$	%T ^b	P^c	$(P;Q)^c$
0	4.187 ^d	0.177 ^c	0	5.918 ^d	0.656 ^e	0	380 ^d	105 ^e
2000	3.948	0.162	1.8	5.361	0.549	3.0	310	85
4000	3.281	0.111	7.1	3.908	0.304	11.9	138	42
6000	2.749	0.072	12.4	2.993	0.190	19.7	53	26
8000	2.428	0.049	16.3	2.444	0.106	24.9	3	13
10000	2.192	0.038	19.0	2.093	0.080	28.7	−22	9
20000	1.703	0.018	26.3	1.358	0.025	37.7	−76	2
50000	1.133	0.005	39.1	0.644	0.004	54.8	−107	0
100000	0.532	0.000	59.5	0.171	0.000	76.5	−79	0
150000	0.218	0.000	76.8	0.037	0.000	90.7	−40	0
200000	0.076	0.000	88.7	0.006	0.000	97.2	−15	0
∞		−39.080575 ^f			−39.065411 ^f			3328 ^g

^a Unless otherwise stated, all energies are reported as errors relative to CCSDT in millihartree.

^b The %T values are the percentages of triples captured during the i -FCIQMC propagations (the $S_z = 1$ triply excited determinants of the B_1 symmetry in the case of the X^3B_1 state and the $S_z = 0$ triply excited determinants of the A_1 symmetry in the case of the A^1A_1 state).

^c Unless otherwise specified, the values of the singlet–triplet gap are reported as errors relative to CCSDT in cm^{-1} .

^d Equivalent to CCSD.

^e Equivalent to CR-CC(2,3) [the most complete variant of CR-CC(2,3) abbreviated sometimes as CR-CC(2,3),D or CR-CC(2,3)_D].

^f Total CCSDT energy in hartree.

^g The CCSDT singlet–triplet gap in cm^{-1} .

TABLE II. Convergence of the $CC(P)$ and $CC(P;Q)$ energies of the $X^1\Sigma_g^+$ state of $(\text{HFH})^-$, as described by the 6-31G(d,p) basis set, at selected H–F distances $R_{\text{H-F}}$ toward their parent CCSDT values. The P spaces used in the $CC(P)$ and $CC(P;Q)$ calculations were defined as all singly and doubly excited determinants and subsets of triply excited determinants extracted from the i -FCIQMC propagations with $\delta\tau = 0.0001$ a.u. The Q spaces used to determine the $CC(P;Q)$ corrections consisted of the triply excited determinants not captured by the corresponding i -FCIQMC runs. The i -FCIQMC calculations preceding the $CC(P)$ and $CC(P;Q)$ steps were initiated by placing 1500 walkers on the RHF reference determinant and the n_a parameter of the initiator algorithm was set at 3. In all post-Hartree–Fock calculations, the lowest core orbital was kept frozen and the spherical components of d orbitals were employed throughout.

MC Iterations	$R_{\text{H-F}} = 1.50 \text{ \AA}$			$R_{\text{H-F}} = 1.75 \text{ \AA}$			$R_{\text{H-F}} = 2.00 \text{ \AA}$			$R_{\text{H-F}} = 2.50 \text{ \AA}$			$R_{\text{H-F}} = 4.00 \text{ \AA}$		
	P^a	$(P;Q)^a$	%T ^b	P^a	$(P;Q)^a$	%T ^b	P^a	$(P;Q)^a$	%T ^b	P^a	$(P;Q)^a$	%T ^b	P^a	$(P;Q)^a$	%T ^b
0	11.412 ^c	−0.343 ^d	0	14.738 ^c	−0.686 ^d	0	17.453 ^c	−1.455 ^d	0	17.051 ^c	−2.800 ^d	0	1.907 ^c	−0.291 ^d	0
2000	2.601	−0.035	34.2	3.998	−0.056	30.5	3.511	−0.110	22.6	6.586	−0.583	15.2	0.412	−0.025	7.6
4000	0.843	−0.028	56.1	1.078	−0.009	49.6	1.979	−0.017	40.5	0.973	−0.050	25.6	0.141	−0.004	11.7
6000	0.595	−0.004	63.9	0.434	−0.003	58.1	0.432	−0.010	46.7	0.459	−0.012	30.2	0.076	−0.003	13.2
8000	0.225	−0.003	68.6	0.477	−0.007	61.4	0.187	−0.003	50.2	0.225	−0.003	33.9	0.037	−0.001	14.4
10000	0.258	−0.003	70.9	0.161	−0.002	63.3	0.136	−0.003	54.5	0.167	0.000	35.4	0.025	−0.001	15.3
20000	0.112	0.000	77.2	0.056	−0.001	71.0	0.079	−0.002	61.1	0.042	−0.001	41.8	0.026	−0.001	19.0
50000	0.017	0.000	88.4	0.019	0.000	85.8	0.005	0.000	77.5	0.009	0.000	58.8	0.002	−0.001	28.6
100000	0.002	0.000	97.7	0.001	0.000	96.3	0.001	0.000	94.4	0.000	0.000	81.8	0.000	0.000	54.8
150000	0.000	0.000	99.5	0.000	0.000	99.4	0.000	0.000	99.2	0.000	0.000	94.1	0.000	0.000	73.7
200000	0.000	0.000	99.9	0.000	0.000	100.0	0.000	0.000	99.9	0.000	0.000	99.2	0.000	0.000	86.9
∞		−100.588130 ^e			−100.576056 ^e			−100.561110 ^e			−100.539783 ^e			−100.525901 ^e	

^a Unless otherwise stated, all energies are reported as errors relative to CCSDT in millihartree.

^b The %T values are the percentages of triples captured during the i -FCIQMC propagations [the $S_z = 0$ triply excited determinants of the $A_g(D_{2h})$ symmetry].

^c Equivalent to CCSD.

^d Equivalent to CR-CC(2,3) [the most complete variant of CR-CC(2,3) abbreviated sometimes as CR-CC(2,3),D or CR-CC(2,3)_D].

^e Total CCSDT energy in hartree.

TABLE III. Convergence of the $CC(P)$ and $CC(P;Q)$ energies of the $A^3\Sigma_u^+$ state of $(HFH)^-$, as described by the 6-31G(d,p) basis set, at selected H–F distances R_{H-F} toward their parent CCSDT values. The P spaces used in the $CC(P)$ and $CC(P;Q)$ calculations were defined as all singly and doubly excited determinants and subsets of triply excited determinants extracted from the i -FCIQMC propagations with $\delta\tau = 0.0001$ a.u. The Q spaces used to determine the $CC(P;Q)$ corrections consisted of the triply excited determinants not captured by the corresponding i -FCIQMC runs. The i -FCIQMC calculations preceding the $CC(P)$ and $CC(P;Q)$ steps were initiated by placing 1500 walkers on the ROHF reference determinant and the n_a parameter of the initiator algorithm was set at 3. In all post-Hartree–Fock calculations, the lowest core orbital was kept frozen and the spherical components of d orbitals were employed throughout.

MC Iterations	$R_{H-F} = 1.50 \text{ \AA}$			$R_{H-F} = 1.75 \text{ \AA}$			$R_{H-F} = 2.00 \text{ \AA}$			$R_{H-F} = 2.50 \text{ \AA}$			$R_{H-F} = 4.00 \text{ \AA}$		
	P^a	$(P;Q)^a$	%T ^b	P^a	$(P;Q)^a$	%T ^b	P^a	$(P;Q)^a$	%T ^b	P^a	$(P;Q)^a$	%T ^b	P^a	$(P;Q)^a$	%T ^b
0	2.268 ^c	-0.217 ^d	0	1.967 ^c	-0.181 ^d	0	1.678 ^c	-0.172 ^d	0	1.277 ^c	-0.167 ^d	0	1.123 ^c	-0.180 ^d	0
2000	0.995	-0.040	27.8	0.826	-0.024	24.2	0.834	-0.038	19.1	0.502	-0.029	10.7	0.239	-0.014	4.5
4000	0.456	-0.010	49.4	0.477	-0.010	41.7	0.475	-0.012	33.7	0.236	-0.009	17.2	0.079	-0.002	5.4
6000	0.338	-0.005	56.4	0.266	-0.001	50.5	0.321	-0.005	41.2	0.174	-0.003	21.5	0.070	-0.003	5.9
8000	0.290	-0.003	60.1	0.254	-0.003	54.2	0.225	-0.003	44.7	0.195	-0.006	23.9	0.064	-0.002	6.0
10000	0.271	-0.003	61.1	0.267	-0.004	56.6	0.201	-0.002	45.7	0.064	-0.003	25.0	0.056	-0.002	6.4
20000	0.201	-0.002	67.9	0.151	-0.001	62.1	0.157	-0.002	52.2	0.078	-0.003	28.6	0.025	-0.001	7.4
50000	0.082	0.000	80.0	0.056	0.000	76.3	0.069	-0.001	66.1	0.049	-0.001	37.4	0.012	0.000	8.4
100000	0.021	0.000	91.8	0.016	0.000	89.4	0.015	0.000	82.8	0.014	0.000	52.9	0.002	0.000	11.7
150000	0.007	0.000	96.7	0.003	0.000	95.8	0.003	0.000	92.9	0.002	0.000	68.6	0.001	0.000	16.8
200000	0.001	0.000	98.8	0.001	0.000	98.4	0.001	0.000	97.1	0.000	0.000	81.8	0.000	0.000	23.8
∞	-100.545633 ^e			-100.554908 ^e			-100.552882 ^e			-100.540435 ^e			-100.526164 ^e		

^a Unless otherwise stated, all energies are reported as errors relative to CCSDT in millihartree.

^b The %T values are the percentages of triples captured during the i -FCIQMC propagations [the $S_z = 1$ triply excited determinants of the $B_{1u}(D_{2h})$ symmetry].

^c Equivalent to CCSD.

^d Equivalent to CR-CC(2,3) [the most complete variant of CR-CC(2,3) abbreviated sometimes as CR-CC(2,3)_D or CR-CC(2,3)_D].

^e Total CCSDT energy in hartree.

TABLE IV. Convergence of the $CC(P)$ and $CC(P;Q)$ singlet–triplet gaps of $(HFH)^-$, as described by the 6-31G(d,p) basis set, at selected H–F distances R_{H-F} toward their parent CCSDT values. The P spaces used in the $CC(P)$ and $CC(P;Q)$ calculations were defined as all singly and doubly excited determinants and subsets of triply excited determinants extracted from the i -FCIQMC propagations with $\delta\tau = 0.0001$ a.u. The Q spaces used to determine the $CC(P;Q)$ corrections consisted of the triply excited determinants not captured by the corresponding i -FCIQMC runs. The i -FCIQMC calculations preceding the $CC(P)$ and $CC(P;Q)$ steps were initiated by placing 1500 walkers on the RHF ($X^1\Sigma_g^+$ state) and ROHF ($A^3\Sigma_u^+$ state) reference determinants and the n_a parameter of the initiator algorithm was set at 3. In all post-Hartree–Fock calculations, the lowest core orbital was kept frozen and the spherical components of d orbitals were employed throughout.

MC Iterations	$R_{H-F} = 1.50 \text{ \AA}$		$R_{H-F} = 1.75 \text{ \AA}$		$R_{H-F} = 2.00 \text{ \AA}$		$R_{H-F} = 2.50 \text{ \AA}$		$R_{H-F} = 4.00 \text{ \AA}$	
	P^a	$(P;Q)^a$	P^a	$(P;Q)^a$	P^a	$(P;Q)^a$	P^a	$(P;Q)^a$	P^a	$(P;Q)^a$
0	2007 ^b	-28 ^c	2803 ^b	-111 ^c	3462 ^b	-282 ^c	3462 ^b	-578 ^c	172 ^b	-24 ^c
2000	353	1	696	-7	588	-16	1335	-122	38	-2
4000	85	-4	132	0	330	-1	162	-9	14	0
6000	56	0	37	0	24	-1	62	-2	1	0
8000	-14	0	49	-1	-8	0	7	1	-6	0
10000	-3	0	-23	0	-14	0	23	0	-7	0
20000	-20	0	-21	0	-17	0	-8	1	0	0
50000	-14	0	-8	0	-14	0	-9	0	-2	0
100000	-4	0	-3	0	-3	0	-3	0	-1	0
150000	-2	0	-1	0	-1	0	0	0	0	0
200000	0	0	0	0	0	0	0	0	0	0
∞	-9327 ^d		-4641 ^d		-1806 ^d		143 ^d		58 ^d	

^a Unless otherwise stated, all singlet–triplet gaps are reported as errors relative to CCSDT in cm^{-1} .

^b Equivalent to CCSD.

^c Equivalent to CR-CC(2,3) [the most complete variant of CR-CC(2,3) abbreviated sometimes as CR-CC(2,3)_D or CR-CC(2,3)_D].

^d The CCSDT singlet–triplet gap in cm^{-1} .

TABLE V. Convergence of the $CC(P)$ and $CC(P;Q)$ energies of the X^1B_{1g} and A^3A_{2g} states of cyclobutadiene, as described by the cc-pVDZ basis set, and of the corresponding vertical singlet–triplet gaps toward their parent CCSDT values. All calculations were performed at the D_{4h} -symmetric transition-state geometry of the X^1B_{1g} state optimized in the MR-AQCC calculations in Ref. 167. The P spaces used in the $CC(P)$ and $CC(P;Q)$ calculations were defined as all singly and doubly excited determinants and subsets of triply excited determinants extracted from the i -FCIQMC propagations with $\delta\tau = 0.0001$ a.u. The Q spaces used to determine the $CC(P;Q)$ corrections consisted of the triply excited determinants not captured by the corresponding i -FCIQMC runs. The i -FCIQMC calculations preceding the $CC(P)$ and $CC(P;Q)$ steps were initiated by placing 1500 walkers on the RHF (X^1B_{1g} state) and ROHF (A^3A_{2g} state) reference determinants and the n_a parameter of the initiator algorithm was set at 3. In all post-Hartree–Fock calculations, the four lowest core orbitals were kept frozen and the spherical components of d orbitals were employed throughout.

MC Iterations	X^1B_{1g}			A^3A_{2g}			$X^1B_{1g} - A^3A_{2g}$	
	P^a	$(P;Q)^a$	%T ^b	P^a	$(P;Q)^a$	%T ^b	P^c	$(P;Q)^c$
0	47.979 ^d	14.636 ^e	0	23.884 ^d	-0.060 ^e	0	15.1 ^d	9.2 ^e
2000	40.663	11.059	3.5	21.004	0.031	3.0	12.3	6.9
4000	27.235	5.921	16.6	14.317	0.068	14.2	8.1	3.7
6000	17.188	2.223	29.5	10.016	0.051	25.5	4.6	1.4
8000	11.207	0.835	39.2	7.463	0.031	34.3	3.3	0.5
10000	8.299	0.429	46.6	5.865	0.020	41.0	1.5	0.3
20000	2.030	0.013	70.0	2.461	0.005	62.8	-0.3	0.0
50000	0.049	0.000	96.9	0.166	0.000	94.2	-0.1	0.0
80000	0.001	0.000	99.9	0.009	0.000	99.6	0.0	0.0
∞		-154.232002 ^f			-154.224380 ^f			-4.8 ^g

^a Unless otherwise stated, all energies are reported as errors relative to CCSDT in millihartree.

^b The %T values are the percentages of triples captured during the i -FCIQMC propagations [the $S_z = 0$ triply excited determinants of the $A_g(D_{2h})$ symmetry in the case of the X^1B_{1g} state and the $S_z = 1$ triply excited determinants of the $B_{1g}(D_{2h})$ symmetry in the case of the A^3A_{2g} state].

^c Unless otherwise specified, the values of the singlet–triplet gaps are reported as errors relative to CCSDT in kcal/mol.

^d Equivalent to CCSD.

^e Equivalent to CR-CC(2,3) [the most complete variant of CR-CC(2,3) abbreviated sometimes as CR-CC(2,3)_D or CR-CC(2,3)_D].

^f Total CCSDT energy in hartree.

^g The CCSDT singlet–triplet gap in kcal/mol.

TABLE VI. Convergence of the $CC(P)$ and $CC(P;Q)$ energies of the $X^3A'_2$ and $A^1E'_2$ states of cyclopentadienyl cation, as described by the cc-pVDZ basis set, and of the corresponding vertical singlet–triplet gaps toward their parent CCSDT values. All calculations were performed at the D_{5h} -symmetric geometry of the $X^3A'_2$ state optimized using the unrestricted CCSD/cc-pVDZ approach in Ref. 118. The P spaces used in the $CC(P)$ and $CC(P;Q)$ calculations were defined as all singly and doubly excited determinants and subsets of triply excited determinants extracted from the i -CISDTQ-MC propagations with $\delta\tau = 0.0001$ a.u. The Q spaces used to determine the $CC(P;Q)$ corrections consisted of the triply excited determinants not captured by the corresponding i -CISDTQ-MC runs. The i -CISDTQ-MC calculations preceding the $CC(P)$ and $CC(P;Q)$ steps were initiated by placing 1500 walkers on the ROHF ($X^3A'_2$ state) and RHF ($A^1E'_2$ state) reference determinants and the n_a parameter of the initiator algorithm was set at 3. In all post-Hartree–Fock calculations, the five lowest core orbitals were kept frozen and the spherical components of d orbitals were employed throughout.

MC Iterations	$X^3A'_2$			$A^1E'_2$			$A^1E'_2 - X^3A'_2$	
	P^a	$(P;Q)^a$	%T ^b	P^a	$(P;Q)^a$	%T ^b	P^c	$(P;Q)^c$
0	28.840 ^d	0.245 ^e	0	38.572 ^d	6.245 ^e	0	6.1 ^d	3.8 ^e
2000	27.396	0.272	0.8	35.598	5.948	1.0	5.1	3.6
4000	22.253	0.267	5.1	27.946	5.078	6.5	3.6	3.0
6000	17.394	0.212	11.6	21.124	3.971	14.7	2.3	2.4
8000	13.743	0.152	18.3	16.042	2.756	23.0	1.4	1.6
10000	11.027	0.108	24.8	12.947	2.248	30.9	1.2	1.3
20000	4.250	0.026	52.1	3.964	0.217	61.4	-0.2	0.1
50000	0.155	0.001	95.3	0.060	0.001	98.3	-0.1	0.0
80000	0.007	0.000	99.8	0.001	0.000	100.0	0.0	0.0
∞		-192.615924 ^f			-192.589235 ^f			16.7 ^g

^a Unless otherwise stated, all energies are reported as errors relative to CCSDT in millihartree.

^b The %T values are the percentages of triples captured during the i -CISDTQ-MC propagations [the $S_z = 1$ triply excited determinants of the $B_2(C_{2v})$ symmetry in the case of the $X^3A'_2$ state and the $S_z = 0$ triply excited determinants of the $A_1(C_{2v})$ symmetry in the case of the $A^1E'_2$ state].

^c Unless otherwise specified, the values of the singlet–triplet gaps are reported as errors relative to CCSDT in kcal/mol.

^d Equivalent to CCSD.

^e Equivalent to CR-CC(2,3) [the most complete variant of CR-CC(2,3) abbreviated sometimes as CR-CC(2,3)_D or CR-CC(2,3)_D].

^f Total CCSDT energy in hartree.

^g The CCSDT singlet–triplet gap in kcal/mol.

TABLE VII. Convergence of the $CC(P)$ and $CC(P;Q)$ energies of the $X^3A'_2$ and B^1A_1 states of trimethylenemethane, as described by the cc-pVDZ basis set, and of the corresponding adiabatic singlet–triplet gaps toward their parent CCSDT values. The D_{3h} - and C_{2v} -symmetric geometries of the $X^3A'_2$ and B^1A_1 states, respectively, optimized in the SF-DFT/6-31G(d) calculations, were taken from Ref. 115. The P spaces used in the $CC(P)$ and $CC(P;Q)$ calculations were defined as all singly and doubly excited determinants and subsets of triply excited determinants extracted from the i -CISDTQ-MC propagations with $\delta\tau = 0.0001$ a.u. The Q spaces used to determine the $CC(P;Q)$ corrections consisted of the triply excited determinants not captured by the corresponding i -CISDTQ-MC runs. The i -CISDTQ-MC calculations preceding the $CC(P)$ and $CC(P;Q)$ steps were initiated by placing 1500 walkers on the ROHF ($X^3A'_2$ state) and RHF (B^1A_1 state) reference determinants and the n_a parameter of the initiator algorithm was set at 3. In all post-Hartree–Fock calculations, the four lowest core orbitals were kept frozen and the spherical components of d orbitals were employed throughout.

MC Iterations	$X^3A'_2$			B^1A_1			$B^1A_1 - X^3A'_2$	
	P^a	$(P;Q)^a$	%T ^b	P^a	$(P;Q)^a$	%T ^b	P^c	$(P;Q)^c$
0	19.202 ^d	0.418 ^e	0	58.051 ^d	13.370 ^e	0	24.4 ^d	8.1 ^e
2000	17.975	0.422	1.1	50.012	9.362	1.2	20.1	5.6
4000	14.462	0.357	6.6	32.925	3.236	7.7	11.6	1.8
6000	11.319	0.253	14.1	20.628	1.260	16.8	5.8	0.6
8000	9.066	0.173	21.3	14.601	0.649	25.5	3.5	0.3
10000	7.429	0.123	27.9	10.680	0.314	33.1	2.0	0.1
20000	3.294	0.031	52.3	2.675	0.028	61.1	−0.4	0.0
50000	0.213	0.001	92.8	0.061	0.000	97.1	−0.1	0.0
80000	0.012	0.000	99.5	0.002	0.000	99.9	0.0	0.0
∞		−155.466242 ^f			−155.431596 ^f			21.7 ^g

^a Unless otherwise stated, all energies are reported as errors relative to CCSDT in millihartree.

^b The %T values are the percentages of triples captured during the i -CISDTQ-MC propagations [the $S_z = 1$ triply excited determinants of the $B_2(C_{2v})$ symmetry in the case of the $X^3A'_2$ state and the $S_z = 0$ triply excited determinants of the A_1 symmetry in the case of the B^1A_1 state].

^c Unless otherwise specified, the values of the singlet–triplet gaps are reported as errors relative to CCSDT in kcal/mol.

^d Equivalent to CCSD.

^e Equivalent to CR-CC(2,3) [the most complete variant of CR-CC(2,3) abbreviated sometimes as CR-CC(2,3)_D or CR-CC(2,3)_D].

^f Total CCSDT energy in hartree.

^g The CCSDT singlet–triplet gap in kcal/mol.

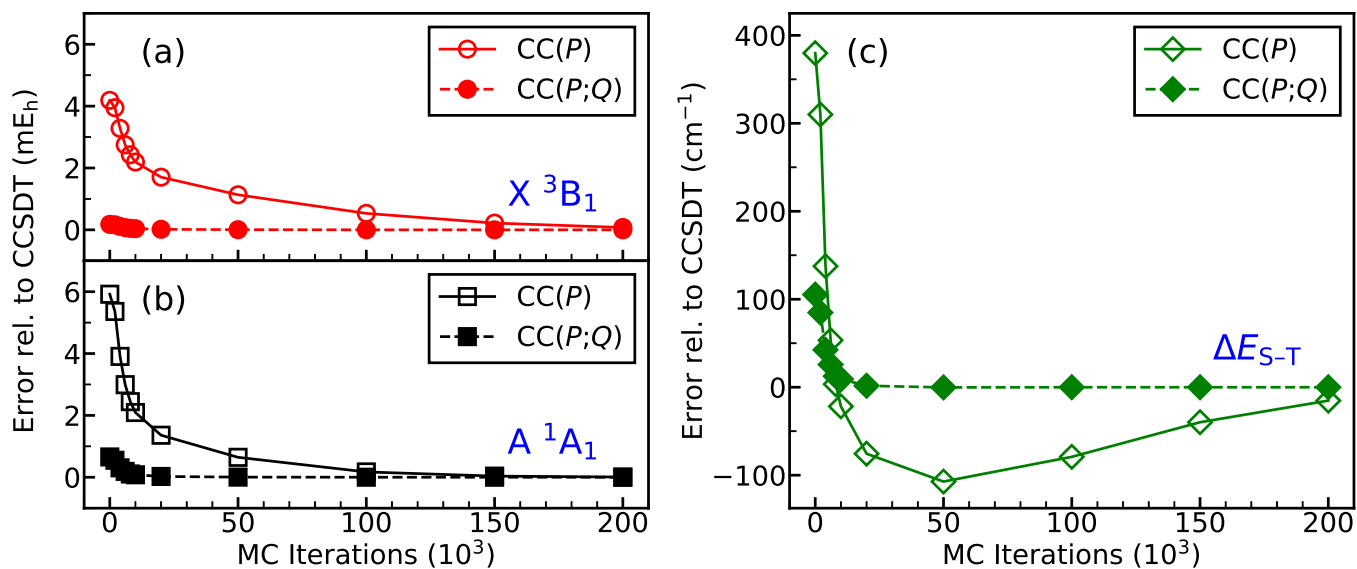


FIG. 1. Convergence of the $CC(P)$ and $CC(P;Q)$ energies of the X^3B_1 [panel (a)] and A^1A_1 [panel (b)] states of methylene, as described by the aug-cc-pVTZ basis set, and of the corresponding adiabatic singlet-triplet gaps [panel (c)] toward their parent CCSDT values. The geometries of the X^3B_1 and A^1A_1 states, optimized in the FCI calculations using the TZ2P basis set, were taken from Ref. 149. The P spaces consisted of all singles and doubles and subsets of triples identified during the i -FCIQMC propagations with $\delta\tau = 0.0001$ a.u. and the Q spaces consisted of the triples not captured by i -FCIQMC.

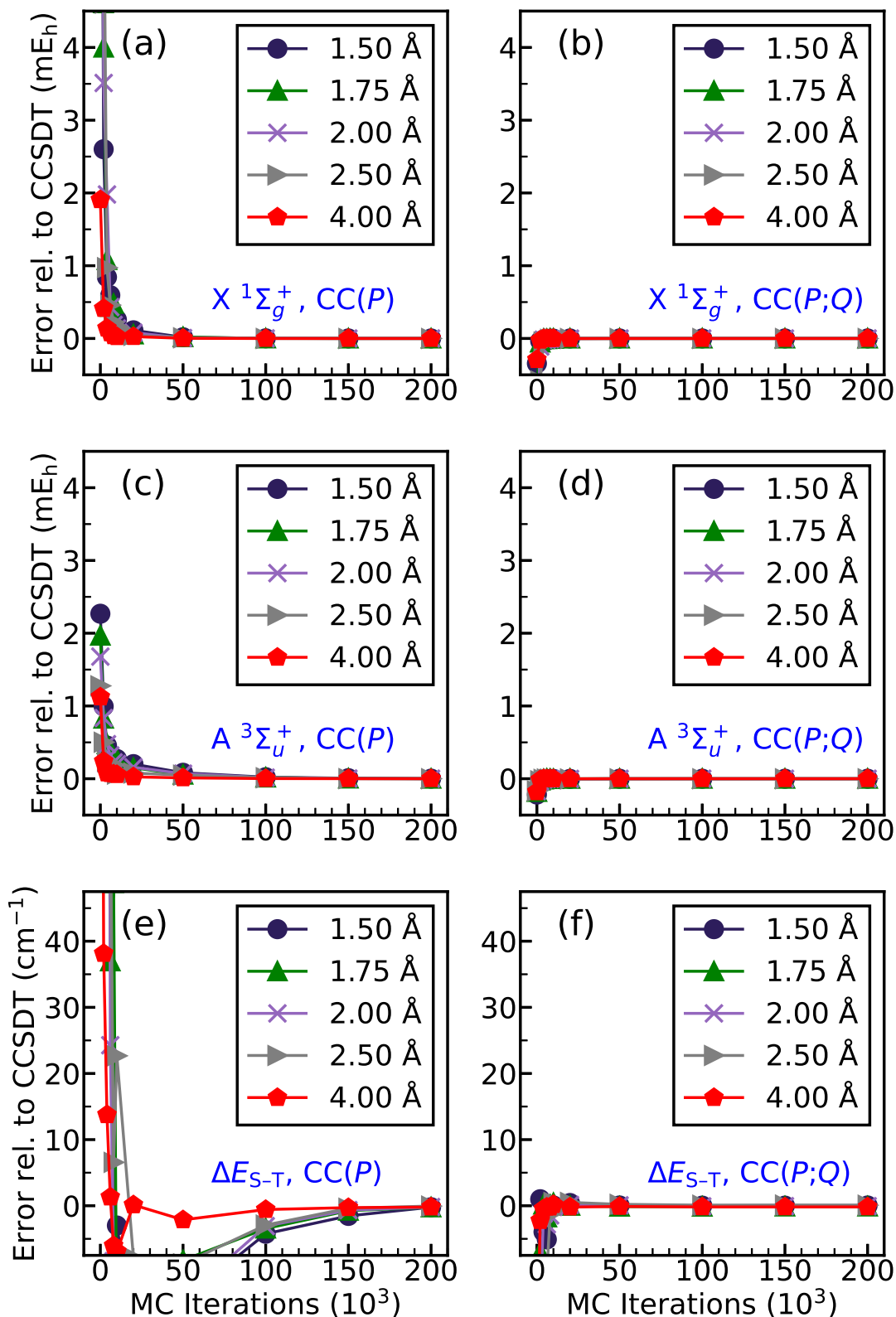


FIG. 2. Convergence of the $CC(P)$ and $CC(P;Q)$ energies of the $X^1\Sigma_g^+$ [panels (a) and (b)] and $A^3\Sigma_u^+$ [panels (c) and (d)] states of $(\text{HFH})^-$, as described by the 6-31G(d,p) basis set, and of the corresponding singlet–triplet gaps [panels (e) and (f)] toward their parent CCSDT values. The H–F distances $R_{\text{H-F}}$ used are 1.50 Å, 1.75 Å, 2.00 Å, 2.50 Å, and 4.00 Å. The P spaces consisted of all singles and doubles and subsets of triples identified during i -FCIQMC propagations with $\delta\tau = 0.0001$ a.u. and the Q spaces consisted of the triples not captured by i -FCIQMC.

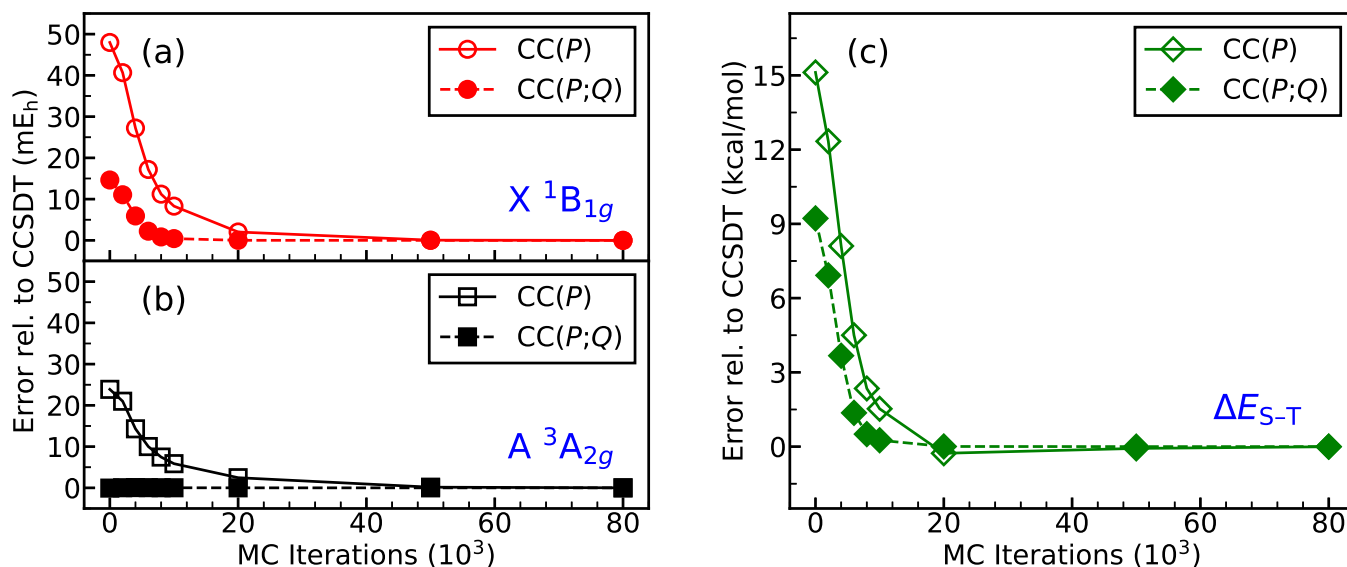


FIG. 3. Convergence of the CC(P) and CC($P;Q$) energies of the X^1B_{1g} [panel (a)] and A^3A_{2g} [panel (b)] states of cyclobutadiene, as described by the cc-pVDZ basis set, and of the corresponding vertical singlet–triplet gaps [panel (c)] toward their parent CCSDT values. All calculations were performed at the D_{4h} -symmetric transition-state geometry of the X^1B_{1g} state optimized in the MR-AQCC calculations in Ref. 167. The P spaces consisted of all singles and doubles and subsets of triples identified during the i -FCIQMC propagations with $\delta\tau = 0.0001$ a.u. and the Q spaces consisted of the triples not captured by i -FCIQMC.

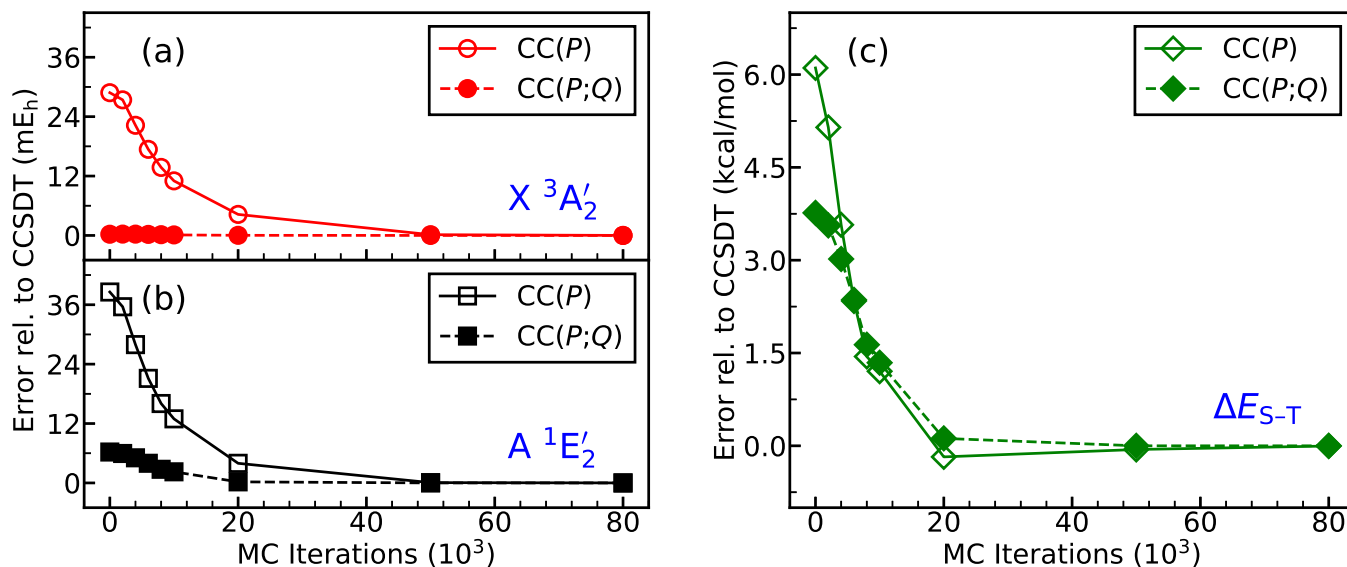


FIG. 4. Convergence of the CC(P) and CC($P;Q$) energies of the $X^3A'_2$ [panel (a)] and $A^1E'_2$ [panel (b)] states of cyclopentadienyl cation, as described by the cc-pVDZ basis set, and of the corresponding vertical singlet–triplet gaps [panel (c)] toward their parent CCSDT values. All calculations were performed at the D_{5h} -symmetric geometry of the $X^3A'_2$ state optimized using the unrestricted CCSD/cc-pVDZ approach in Ref. 118. The P spaces consisted of all singles and doubles and subsets of triples identified during the i -CISDTQ-MC propagations with $\delta\tau = 0.0001$ a.u. and the Q spaces consisted of the triples not captured by i -CISDTQ-MC.

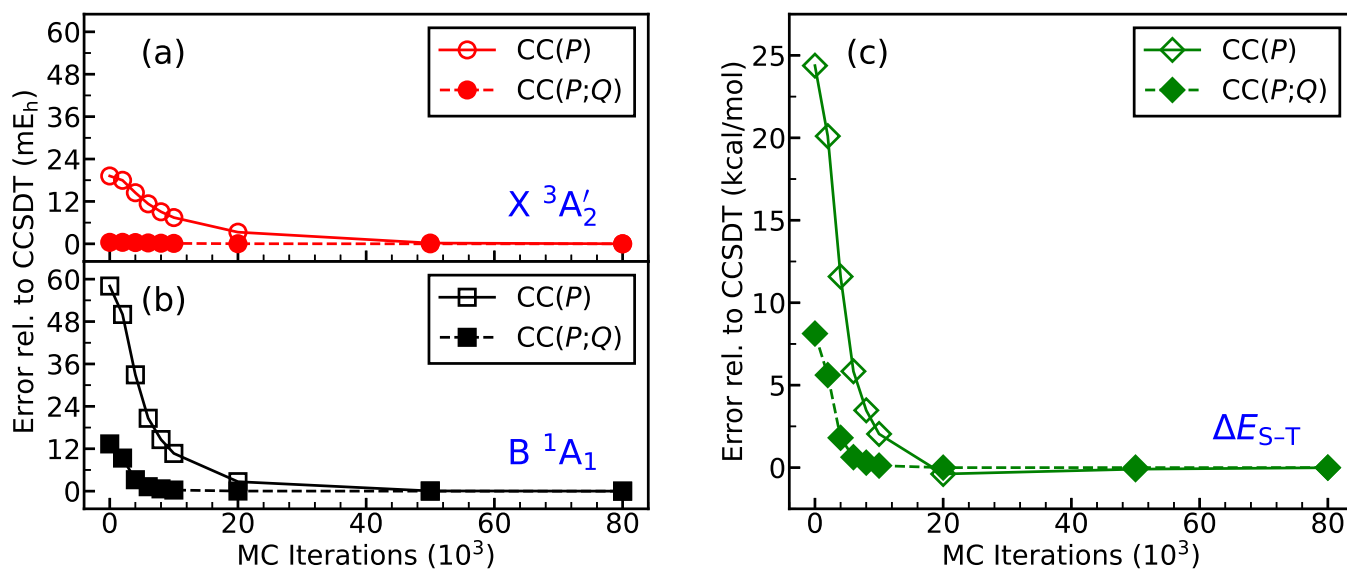


FIG. 5. Convergence of the CC(P) and CC($P;Q$) energies of the X ³A'₂ [panel (a)] and B ¹A₁ [panel (b)] states of trimethylenemethane, as described by the cc-pVDZ basis set, and of the corresponding adiabatic singlet–triplet gaps [panel (c)] toward their parent CCSDT values. The geometries of the X ³A'₂ and B ¹A₁ states, optimized in the SF-DFT/6-31G(d) calculations, were taken from Ref. 115. The P spaces consisted of all singles and doubles and subsets of triples identified during the i -CISDTQ-MC propagations with $\delta\tau = 0.0001$ a.u. and the Q spaces consisted of the triples not captured by i -CISDTQ-MC.